NASA CONTRACTOR REPORT

NASA CR-2379

NASA CR-2379

SENSITIVITY ANALYSIS OF TORSIONAL VIBRATION CHARACTERISTICS OF HELICOPTER ROTOR BLADES

Part I - Structural Dynamics Analysis

by Theodore Bratanow and Akin Ecer

Prepared by
UNIVERSITY OF WISCONSIN-MILWAUKEE
Milwaukee, Wis.
for Langley Research Center

NATIONAL AERONAUTICS AND SPACE ADMINISTRATION • WASHINGTON, D. C. • MARCH 1974

For sale by the National Technical Information Service, Springfield, Virginia 22151

1. Report No.	2. Government Accession No.	3. Recipient's Catalog No.
NASA CR-2379		

SENSITIVITY ANALYSIS OF TORSIONAL VIBRATION CHARACTERISTICS OF HELICOPTER ROTOR BLADES - PART I. STRUCTURAL DYNAMICS ANALYSIS	5. Report Date March 1974 6. Performing Organization Code
7. Author(s) THEODORE BRATANOW AND AKIN ECER	8. Performing Organization Report No. 10. Work Unit No.
9. Performing Organization Name and Address UNIVERSITY OF WISCONSIN - MILWAUKEE MILWAUKEE, WISCONSIN	11. Contract or Grant No. NGR 50-007-001
12. Sponsoring Agency Name and Address NATIONAL AERONAUTICS AND SPACE ADMINISTRATION WASHINGTON, D.C. 20546	13. Type of Report and Period Covered CONTRACTOR REPORT 14. Sponsoring Agency Code

15. Supplementary Notes

TOPICAL REPORT

16. Abstract

A THEORETICAL INVESTIGATION OF STRUCTURAL VIBRATION CHARACTERISTICS OF ROTOR BLADES WAS CARRIED OUT. COUPLED EQUATIONS OF MOTION FOR FLAPWISE BENDING AND TORSION WERE FORMULATED FOR ROTOR BLADES WITH NONCOLLINEAR ELASTIC AND MASS AXES. THE FINITE ELEMENT METHOD WAS APPLIED FOR A DETAILED REPRESENTATION OF BLADE STRUCTURAL PROPERTIES. COUPLED STRUCTURAL MASS AND STIFFNESS COEFFICIENTS WERE EVALUATED. THE RANGE OF VALIDITY OF A SET OF COUPLED EQUATIONS OF MOTION LINEARIZED WITH RESPECT TO ECCENTRICITY BETWEEN ELASTIC AND MASS AXES WAS INVESTIGATED. THE SENSITIVITY OF BLADE VIBRATION CHARACTERISTICS TO TORSION WERE EVALUATED BY VARYING BLADE GEOMETRIC PROPERTIES, BOUNDARY CONDITIONS, AND ECCENTRICITIES BETWEEN MASS AND ELASTIC AXES.

17. Key Words (Suggested by Author(s))	18. Distribution Statement
ROTOR BLADE DYNAMICS FINITE ELEMENT METHOD COUPLED RESPONSE TORSIONAL COUPLING	UNCLASSIFIED - UNLIMITED Cat. 32

19. Security Classif. (of this report)	20. Security Classif. (of this page)	21. No. of Pages	22. Price
UNCLASSIFIED	UNCLASSIFIED	46	$3.00

CONTENTS

TABLES

ILLUSTRATIONS

SENSITIVITY ANALYSIS OF TORSIONAL VIBRATION CHARACTERISTICS OF HELICOPTER ROTOR BLADES

PART I - STRUCTURAL DYNAMICS ANALYSIS

By Theodore Bratanow* and Akin Ecer**
University of Wisconsin-Milwaukee

SUMMARY

A theoretical investigation of structural vibration characteristics of rotor blades was carried out. Coupled equations of motion for flapwise bending and torsion were formulated for rotor blades with non-collinear elastic and mass axes. The finite element method was applied for a detailed representation of blade structural properties. Coupled structural mass and stiffness coefficients were evaluated. The range of validity of a set of coupled equations of motion linearized with respect to eccentricity between elastic and mass axes was investigated. The sensitivity of blade vibration characteristics to torsion were evaluated by varying blade geometric properties, boundary conditions, and eccentricities between mass and elastic axes.

INTRODUCTION

A complete analysis of the dynamic response of helicopter rotor blades under actual flight conditions is difficult because of the three-dimensional nature of both blade deformations and unsteady flow around the blades. Higher operational forward speed and maneuverability requirements for modern helicopters have further increased the complexity of the problem. As indicated by theoretical and experimental studies, at higher tip-speed ratios the blade dynamic response characteristics become increasingly sensitive to torsional oscillation.

The objective of the conducted investigation was to evaluate the effect of torsional oscillations on blade dynamic response characteristics and to analyze the sensitivity of torsional oscillations to blade aerodynamic, structural, and geometric properties. In the first part of the analysis, the coupled equations of torsional and bending motion of a rotating blade with non-collinear elastic and mass axes were developed in finite element form considering only structural parameters. The results from this formulation were compared with results from a system of differential equations of motion derived by Houbolt and Brooks for the same problem [1]. The importance of the second order terms in eccentricity between mass and elastic axes was established. The obtained overall results were also compared with results obtained by Isakson and Eisley [2].

---

* Professor, ** Assistant Professor, Department of Mechanics, College of Engineering and Applied Science.

SYMBOLS

a_i	a scalar
A_i, B_{ij}, C_{ij}, D_j, E_j, H_j	generalized coupled mass and stiffness terms (see Eq. (A13))
b_j	a scalar
e_i	a scalar
EI	bending stiffness of a blade, N-m^2
f_i	a scalar
h	vertical displacement of a blade at the elastic center, m.
$\underline{h}$	column vector representing bending displacements
h_G	vertical displacement of a blade at the center of mass, m.
$\underline{h}_i$	eigenvector of Eq. (B3)
h_i	eigenfunction corresponding to the bending displacement component of $\underline{p}_i$, m.
I_θ	torsional inertia of the rotor blade, N-sec.^{2}
$\underline{I}$	identity matrix
JG	torsional stiffness of a blade, N-m^2
$\underline{K}$	total stiffness matrix
$\underline{K}_i$	total stiffness matrix of an element
$\underline{K}_B$	stiffness matrix in bending
$\underline{K}_C$	coupled stiffness matrix
$\underline{K}_T$	stiffness matrix in torsion
$\underline{K}_{T_i}$	stiffness matrix in torsion for a blade element

ℓ	length of blade element, m.
m	mass of the blade per unit length, N-sec.^{2}/m^2
$\underline{M}$	total mass matrix
$\underline{M}_i$	total mass matrix of an element
$\underline{M}_B$	mass matrix in bending
$\underline{M}_C$	coupled mass matrix
$\underline{M}_T$	mass matrix in torsion
$\underline{M}_{T_i}$	mass matrix in torsion for a blade element
P	a scalar (see Eq. (A21))
$\underline{P}$	column vector defining nodal forces in bending
q	a scalar (see Eq. (A21))
R	rotor radius, m.
S	non-dimensional eccentricity, $S = x_\theta^2\, m/I_\theta$
S_1	non-dimensional eccentricity (see Eq. (A21))
S_2	non-dimensional eccentricity (see Eq. (A21))
S_{ki}	generalized coupled bending damping in torsion, N-sec./rad
t	time variable
T	centrifugal force along the longitudinal axis of a rotating blade, N
U	total energy for coupled bending and torsion, N-m
U_B	total energy in bending, N-m
U_T	total energy in torsion, N-m
x	distance on the longitudinal axis of cantilever blade from the fixed end, m.
x_θ	eccentricity between the elastic and mass center, m.

γ	a scalar
$\underline{\delta}$	column vector representing bending and torsional displacements of a blade
ζ	non-dimensionalized abscissa of a point on a blade element
θ	pitch change due to blade torsion, rad
$\underline{\theta}$	column vector representing torsional rotations
θ_i	torsional rotation of a blade at the i^{th} mode, rad
λ	square of the ratio of lowest torsional frequency to lowest bending frequency
η	ratio of torsional rotations to bending displacements in the vibration mode corresponding to the lowest frequency, rad/m.
$\underline{\rho}$	column vector representing bending displacements
ω	coupled frequency of the blade, rad/sec.
Ω	angular velocity of a rotating blade, rad/sec.
ω_B	natural frequency of a blade in bending, rad/sec.
ω_{B_i}	lowest coupled frequency corresponding to a predominantly bending mode, rad/sec.
ω_T	natural frequency of a blade in torsion, rad/sec.
ω_{T_i}	lowest coupled frequency corresponding to a predominantly torsional mode, rad/sec.

Superscript

t	transpose

THE ANALYSIS OF STRUCTURAL VIBRATION CHARACTERISTICS OF ROTOR BLADES

Method of Solution

The energy method was applied in formulating the coupled equations of motion for helicopter rotor blades in flapwise bending and torsion. The formulation is similar to the one used by Garland [3] for analyzing non-rotating beams. The details of the mathematical analysis are given in Appendix A.

The coupled vibration characteristics of a rotating blade can be analyzed by first calculating the generalized coupled mass, damping, and stiffness coefficients in Eq. (A13) and then solving Eqs. (A11) and (A12). A coupled set of equations of motion, (B1), was formulated as shown in Appendix B. A discretized set of mass and stiffness matrices was developed in finite element form. The derivation of each of the matrices in the set of matrix differential equations is given in Appendix C.

A numerical method was applied for the solution in Eqs. (A11) and (A12). The following characteristics were established:

- coupled structural vibration characteristics of rotor blades in bending and torsion
- stability characteristics of the equations of Houbolt and Brooks.

Variation of Coupled Vibration Characteristics with Eccentricity between Elastic and Mass Axes

The variation of blade frequencies with increasing eccentricity between elastic and mass axes can be analysed from Eq. (A21). This analysis is described in Appendix A. The variation of the frequencies of the sample blade for a two-degree-of-freedom system is illustrated in figure 1. As can be seen, when the non-dimensionalized eccentricity parameter S increases, the lower of the two frequencies corresponding to a predominantly bending mode decreases slightly, while the torsional frequency increases.

A further consideration of figure 1 indicates the main features of the coupled structural behavior of a rotating blade, which can be summarized as follows:

a) for values of the eccentricity x_θ equal to zero (S = 0) uncoupled bending and torsional frequencies correspond to q = 1 and q = λ, respectively. As the coupling increases, the frequency corresponding to a predominantly bending mode decreases, while the torsional frequency increases. As can be seen from the left portion of the curve, the bending frequencies are bound between

$$\omega_{B_1}^2 > \omega^2 > \Omega^2 \tag{1}$$

b) the left portion of the curve can be approximated by a straight line as follows:

$$q \sim 1 - \gamma S \tag{2}$$

The ratio of torsional rotations to bending displacements can be calculated from Eqs. (A18) and (A19) as

$$\eta^2 = \left(\frac{b_1 f_1}{a_1 e_1} \right)^2 = \frac{\omega_{B_1}^2 - \omega^2}{\omega_{T_1}^2 \omega^2 + S(\Omega^2 - \omega^2)} \frac{m}{I_\theta} \tag{3}$$

Observing also that

$$\omega_{T_1}^2 >> \omega^2 \tag{4}$$

and

$$\eta^2 = \frac{m}{I_\theta} \frac{\omega_{B_1}^2 \gamma}{\omega_{T_1}^2} S \tag{5}$$

the ratio of coupling between torsional and bending modes is

$$\eta \propto \frac{m\omega_{B_1}}{I_\theta \omega_{T_1}} x_\theta \tag{6}$$

Considering the left portion of the curve in figure 1, one can deduce from Eq. (6) that the coupling effect increases linearly with increasing eccentricity.

Stability of the Set of Linearized Coupled Equations of Motion of Rotor Blades

A set of equations of motion describing the vibrational behavior of a rotor blade has been developed by Houbolt and Brooks [1] in the following form:

$$\left(EIh''\right)'' - \left(Th'\right)' - \left(mx\Omega^2 x_\theta \theta'\right)' + m\left(\ddot{h} + x_\theta \ddot{\theta}\right) = 0 \qquad (7)$$

$$\left(JG\theta'\right)' + mx\Omega^2 x_\theta h' + \Omega^2 I_\theta \theta + I_\theta \ddot{\theta} + mx_\theta \ddot{h} = 0 \qquad (8)$$

Eqs. (7) and (8) have been used by several investigators for calculating dynamic response of rotor blades [2,4]. These equations represent a linearized form of Eqs. (A11) and (A12) with respect to x_θ; only the first order terms of x_θ being considered. The second order terms E_j and H_j correspond to the change in moment of inertia of the blade and change in the position of the axial force due to x_θ, respectively.

In this portion of the work the effect of linearization of Eqs. (7) and (8) was investigated in two steps:

a) stability of the system of linearized Eqs. (7) and (8)

b) comparative evaluation of approximations in Eqs. (A11) and (A12).

The sensitivity of frequencies to eccentricity between elastic and mass axes was calculated from Eqs. (7) and (8). Neglecting the higher order terms of x_θ in Eqs. (A18) and (A19), these equations can be written in matrix form as follows:

$$\left\{ \begin{bmatrix} \omega_B^2 & x_\theta \Omega^2 \\ x_\theta \Omega^2 & \frac{I_\theta}{m} \omega_T^2 \end{bmatrix} - \omega^2 \begin{bmatrix} 1 & x_\theta \\ x_\theta & \frac{I_\theta}{m} \end{bmatrix} \right\} \begin{bmatrix} a_1 e_1 \\ b_1 f_1 \end{bmatrix} = 0 \qquad (9)$$

The dynamic system represented by Eq. (9) can be defined in terms of mass and stiffness matrices as

$$[\underline{K} - \omega^2 \underline{M}]\ \underline{\delta} = [0] \qquad (10)$$

The stability of the system represented by Eq. (10) can be determined by ascertaining whether the mass and stiffness matrices are positive definite. For Eq. (1) one can show that

$$\frac{x_\theta^2 m}{I_\theta} < 1 \qquad \det [M] > 0 \qquad (11)$$

$$\frac{x_\theta^2 m}{I_\theta} < \frac{\omega_{T_1}^2 \omega_{B_1}^2}{\Omega^4} \qquad \det [K] > 0 \qquad (12)$$

Since

$$\frac{\omega_{T_1}^2 \; \omega_{B_1}^2}{\Omega^4} > 1, \tag{13}$$

the rotor blade vibrations become unstable in the respective first torsional and bending modes, if

$$\frac{x_\theta^2 m}{I_\theta} > 1. \tag{14}$$

The eigenvalues of Eq. (10) can be calculated from the following equation:

$$\det \left[\underline{M}^{-1}\underline{K} - \omega^2 \underline{I} \right] = \frac{1}{1-S_2} \left[(\lambda-q)\,(1-q) \; - \; S_2(q-p)^2 \right] = 0 \tag{15}$$

The non-dimensionalized eccentricity between mass and elastic axes related to the non-dimensionalized coupled frequency is shown in figure 2. Several conclusions about the coupled behavior can be derived from the curve shown in figure 2. From a comparison of Eq. (A21) and Eq. (15) it follows that

$$S_1 = \frac{(1-q)(\lambda-q)}{(p-q)(p-1)} \qquad \text{and} \qquad S_2 = \frac{(\lambda-q)(1-q)}{(p-q)(p-q)} \tag{16}$$

From Eq. (16) one can derive the relation

$$\frac{S_1}{S_2} = \frac{p-q}{p-1} \tag{17}$$

Thus, one can conclude that the solution of Eq. (15) is satisfactory for the left portion of the curve in figure 2. However, there is an important difference for the right portion of the curve, since S_1/S_2 is not close to unity.

The following conclusions can be deduced from the above results:

a) the values of the lower coupled frequencies obtained from the Houbolt and Brooks equations would be satisfactory

b) Eqs. (7) and (8) become unstable when there is a small increase in eccentricity between the mass and elastic axes.

Such results are significant for the numerical integration of the equations of motion. Instability of these equations leads to large torsional displacements and thus to the conclusion that the actual system is unstable.

Coupled Vibration Analysis of a Sample Rotor Blade

A sample rotor blade was chosen to illustrate the coupled vibration behavior. The finite element method, described in Appendices B and C, was applied for the numerical analysis. The structural properties of the sample blade are listed in table 1. The uncoupled frequencies shown in table 2, were calculated using the numerical procedure summarized in Appendices B and C. The mode shapes for uncoupled vibrations are illustrated in figure 3. The coupled torsional behavior of the sample blade was then analyzed.

Stability of the Houbolt and Brooks equations for the sample blade - The analysis described in Appendix B was applied for determining the stability of the Houbolt and Brooks equations; checking where the torsional modes become unstable. Considering only two-degrees-of-freedom for the sample blade, one can evaluate the critical eccentricity from

$$x_\theta^2 = \frac{A_1 D_1}{C_{11}^2}, \qquad x_\theta = 0.089 \tag{18}$$

For a four-degree-of-freedom system (two in bending and two in torsion), a quadratic expression was derived from the determinant of Eq. (B11) for determining the critical eccentricity. The quadratic equation is

$$A_1 A_2 D_1 D_2 - x_\theta^2 \left[A_1 (C_{22}^2 D_1 + C_{12}^2 D_2) + A_2 (C_{11}^2 D_2 + C_{21}^2 D_1) \right] - x_\theta^4 \left[C_{11} C_{22} - C_{21} C_{12} \right] = 0 \tag{19}$$

From Eq. (19) the value of the critical eccentricity is obtained as

$$x_\theta = 0.057 \tag{20}$$

The variation of coupled frequencies with increasing eccentricity was computed from the procedure described in Appendices B and C. The obtained numerical results for a two-degree-of-freedom system are shown in figures 4 and 5 and listed in table 3. The variation of frequency with increasing eccentricity agrees with the results predicted by Eqs. (16) and (17). Although the bending frequencies are quite accurate, the torsional frequencies can show considerable deviation. The instability of the torsional mode, as indicated in figure 5, agrees with the results from Eq. (18). For a multi-degree-of-freedom system the critical eccentricity that causes instability was found to be in the range of

$$0.050 < x_\theta < 0.061 \tag{21}$$

These results agree with the results obtained from the two-degree-of-freedom system in Eq. (19). Thus, for the sample blade the equations of Houbolt and Brooks may become unstable for moderate eccentricities. One has to be careful when using such equations as a numerical integration basis for the determination of the response of rotor blades. On the other hand, if desired, the second order terms in x_θ can be included quite conveniently in the analysis by using the finite element formulation.

Effect of blade support conditions - The sample blade was analyzed with an assumed hinged support, which allows flapwise rotations. The calculated frequencies for the lowest modes and for various blade rotational speeds are presented in figure 6. The sample blade was also analyzed for a fixed-end boundary condition, in flapwise bending. The vibration frequencies for this case are presented in figure 7 and compared with the frequencies of a hinged blade as shown in figure 8.

The coupled mode shapes of both hinged and fixed blades are shown in figures 10 and 11. As the end-fixity of the blade against bending rotation is increased, the bending stiffness increases; thus, the frequencies become correspondingly higher. The torsional component of the lowest coupled mode is also increased.

Effect of eccentricity between mass and elastic centers - As shown in figure 7, the lowest coupled frequency is affected by increasing the eccentricity between mass and elastic axes for the fixed blade; however, this frequency is less affected for the hinged blade. Frequencies corresponding to bending and torsional modes are compared for different eccentricities as shown in figure 12. Such results agree with the previously described results on the variation of frequencies with increasing eccentricity. The torsional component of the lowest coupled mode is plotted for different eccentricities in figure 12. The results also show the linear relationship between eccentricity and the degree of coupling observed in Eq. (6).

Effect of rotational speed - The variation of frequency with increasing blade rotational speed for different boundary conditions and varying eccentricities is shown in figures 6, 7, 8, and 12. As can be seen from these figures, the square of the coupled frequency term is linearly proportional to the square of the rotational velocity.

The torsional rotation at the blade tip is plotted in figure 9 for various eccentricities at different rotational speeds. From the plotted curves one can observe that the torsional coupled motion increases linearly with eccentricity. For constant eccentricities this motion is also proportional to the square of the blade rotational speed.

Effect of blade structural properties on coupled torsional behavior - It was shown that an approximate relationship, Eq. (20), existed for the coupled motion of rotor blades in bending and torsion. The validity of this relationship was examined by varying each of the parameters in the equation. The sensitivity of the torsional coupling parameter η with respect to each of the parameters was also checked for a multi-degree-of-freedom system.

When the distribution of the blade weight was uniformly increased by 30%, it was found that the bending and torsional frequencies decreased; the first bending frequency by 1.5% and the first torsional frequency by 2.3%. In accordance with Eq. (A20), the increase of the m/I_θ ratio resulted in an increased coupling of the response. As shown in figure 13 the torsional displacements increased by 30%. It appears then that the torsional coupling is quite sensitive to weight changes.

Increasing the torsional inertia by 30% resulted in no change in the lowest bending frequency; however, the torsional frequency decreased as shown in figure 15. As shown in figure 14, there was also an increase in coupled torsional rotation in the second mode; however, there was no effect on the first mode. Such results can also be obtained from Eq. (A20). The increased torsional inertia and the resulting decrease in torsional frequency has a balancing effect; producing no increase in coupling. The effect of decreasing torsional frequency is significant for the modes above the first bending mode and causes a net increase as shown in figure 14.

The effect of an increase in the torsional rigidity on the frequencies and the mode shapes is presented in figures 16 and 17. Increasing the torsional rigidity by 30% led to a 25% reduction of the maximum torsional rotation in the first coupled mode. The lower coupled frequency was not affected, although the predominantly torsional frequencies increased. The plotted results correspond to Eq. (A20); showing an increase in torsional frequency and a decrease in the torsional component of the lowest coupled mode.

Increasing the bending inertia by 30% resulted in no significant change in the bending and torsional frequencies or in the respective mode shapes. The results confirm again the validity of Eq. (A20), since coupling is not affected by a variation of the bending inertia.

Concluding Remarks

The presented analysis extends the application of the equations of motion of Houbolt and Brooks for consideration of larger eccentricities between rotor blade elastic and mass axes. The presented results indicate the significance of individual structural parameters in determining the sensitivity of coupled bending and torsional vibration characteristics.

The results obtained for the sample blade show that for a rigorous analysis of vibration response characteristics, one should consider that:

- the blade boundary conditions are important when determining the coupling ratio of torsional to bending displacements
- the degree of coupling is linearly proportional to the square of the eccentricity between the elastic and mass axes

a more accurate representation of mass and stiffness properties is required for the coupled analysis of bending and torsion.

When a detailed representation of the significant parameters is available, the blade sensitivity analysis can be used as a means of improving blade vibration and stability characteristics.

APPENDIX A

DERIVATION OF THE EQUATIONS OF MOTION OF A ROTATING BLADE IN FLAPWISE BENDING AND TORSION

The total energy of the blade, when coupling is not considered, consists of

$$U_B = \frac{1}{2} \int_0^R (EIh''^2 - \omega_B^2 mh^2 + Th'^2)\, dx \tag{A1}$$

for bending motion and

$$U_T = \frac{1}{2} \int_0^R (JG\theta'^2 - \omega_T^2 I_\theta \theta^2 + \Omega^2 I_\theta \theta^2)\, dx \tag{A2}$$

for torsional motion.

For the coupled motion of the blade the displacements at the center of mass of the blade can be defined as

$$h_G = h + x_\theta \theta \tag{A3}$$

whereby Eq. (A3) is valid only for small values of θ.

The potential energy for the coupled motion can be expressed as

$$U = \frac{1}{2} \int_0^R (EIh''^2 - \omega^2 mh_G^2 + Th_G'^2 + JG\theta'^2 - \omega^2 I_\theta \theta^2 + \Omega^2 I_\theta \theta^2)\, dx \tag{A4}$$

Substituting Eqs. (A1), (A2), and (A3) in Eq. (A4), one can obtain:

$$U = \frac{1}{2} \int_0^R \Big[(\omega_B^2 - \omega^2) mh^2 + (\omega_T^2 - \omega^2) I_\theta \theta^2 - \omega^2 m\theta^2 x_\theta^2 - \omega^2 m\theta x_\theta h + Tx_\theta^2 \theta'^2 + 2Tx_\theta \theta' h' \Big]\, dx + U_B + U_T \tag{A5}$$

For the bending and torsional displacements one can assume the following functions:

$$h = \sum_{i=1}^{\infty} a_i h_i \tag{A6}$$

$$\theta = \sum_{j=1}^{\infty} b_j \theta_j \tag{A7}$$

where the displacement functions h_i and θ_j represent eigenvectors of the uncoupled Eqs. (A1) and (A2). One can also write

$$U_B = \frac{1}{2} \sum_i a_i^2 \int_o^R \left[EIh_i''^2 - \omega_B^2 m h_i^2 + Th_i'^2 \right] dx \tag{A8}$$

and apply the principle of minimum energy to obtain

$$\frac{\partial U_B}{\partial a_i} = 0 \tag{A9}$$

For torsional motion one can similarly write

$$\frac{\partial U_T}{\partial b_j} = 0 \tag{A10}$$

Substituting Eqs. (A6) and (A7) in Eq. (A5), and considering the results of Eqs. (A9) and (A10), according to the principle of minimum energy

$$a_i (\omega_{B_i}^2 - \omega^2) A_i - x_\theta b_j \left[\Omega^2 B_{ij} - \omega^2 C_{ij} \right] = 0 \tag{A11}$$

$$b_j (\omega_{T_j}^2 - \omega^2) D_j - x_\theta a_i \left[\Omega^2 B_{ij} - \omega^2 C_{ij} \right] - \omega^2 x_\theta^2 E_j + \Omega^2 x_\theta^2 H_j = 0 \tag{A12}$$

where

$$A_i = \int_o^R m h_i^2 \, dx, \qquad B_{ij} = \frac{1}{\Omega^2} \int_o^R T \theta_j' h_j' \, dx,$$

$$C_{ij} = \int_o^R mh_i\theta_j \, dx, \qquad D_j = \int_o^R I_\theta \theta_j^2 \, dx,$$

$$E_j = \int_o^R m\theta_j^2 \, dx, \qquad H_j = \frac{1}{\Omega^2} \int_o^R T\theta_j'^2 \, dx \tag{A13}$$

It is now possible to calculate the generalized coefficients (A_i, B_{ij}, C_{ij}, D_j, E_j, H_j) and to investigate the effects of the coupling.

An approximate investigation can be carried out when one considers the first bending mode and the first torsional mode of a rotating blade; i.e., for i = 1 and j = 1, Eqs. (A11) and (A12) become

$$a_1(\omega_{B_1}^2 - \omega^2) A_1 - x_\theta b_1 \left[\Omega^2 B_{11} - \omega^2 C_{11} \right] = 0 \tag{A14}$$

$$b_1(\omega_{T_1}^2 - \omega^2) D_1 - x_\theta a_1 \left[\Omega^2 B_{11} - \omega^2 C_{11} \right] - \omega^2 x_\theta^2 E_1 + \Omega^2 x_\theta^2 H_1 = 0 \tag{A15}$$

The lowest uncoupled modes in bending and torsion, respectively, of a rotating blade of uniform cross section can be approximated as

$$h_1 = e_1 x \tag{A16}$$

$$\theta_1 = f_1 x \tag{A17}$$

For a rotor blade of uniform cross section and uniform eccentricity along the blade, Eqs. (A14) and (A15) become

$$(\omega_{B_1}^2 - \omega^2) ma_1 e_1 + (\Omega^2 - \omega^2) mx_\theta b_1 f_1 = 0 \tag{A18}$$

$$(\Omega^2 - \omega^2) mx_\theta a_1 e_1 + \left\{ (\omega_{T_1}^2 - \omega^2) I_\theta + mx_\theta^2 (\Omega^2 - \omega^2) \right\} b_1 f_1 = 0 \tag{A19}$$

From Eqs. (A18) and (A19) we can now write

$$\frac{x_\theta^2 m}{I_\theta} = \frac{\left(\frac{\omega^2}{\omega_{B_1}^2} - 1 \right) \left(\frac{\omega^2}{\omega_{B_1}^2} - \frac{\omega_{T_1}^2}{\omega_{B_1}^2} \right)}{\left(\frac{\Omega^2}{\omega_{B_1}^2} - \frac{\omega^2}{\omega_{B_1}^2} \right) \left(\frac{\Omega^2}{\omega_{B_1}^2} - 1 \right)} \tag{A20}$$

The expression (A20) can be represented as

$$S_1 = \frac{(q-1)\ (q-\lambda)}{(p-q)\ (p-1)} \tag{A21}$$

APPENDIX B

FINITE ELEMENT FORMULATION OF THE LINEARIZED EQUATIONS OF HOUBOLT AND BROOKS

A general solution to the equations of Houbolt and Brooks can be obtained by formulating the equations in matrix form and then applying the finite element theory. These equations can be written in general form as follows:

$$\left\{ -\omega^2 \begin{bmatrix} \underline{M}_B & x_\theta \underline{M}_C \\ x_\theta \underline{M}_C^t & \underline{M}_T \end{bmatrix} + \begin{bmatrix} \underline{K}_B & x_\theta \underline{K}_C \\ x_\theta \underline{K}_C^t & \underline{K}_T \end{bmatrix} \right\} \begin{bmatrix} \underline{h} \\ \underline{\theta} \end{bmatrix} = 0 \qquad \text{(B1)}$$

The formulation of the matrices in Eq. (B1) is given in Appendix C. Total energy of the blade can be expressed in matrix form as follows:

$$U = -\frac{1}{2}\omega^2 \left[\underline{h}^t \underline{M}_B \underline{h} + x_\theta \underline{\theta}^t \underline{M}_C^t \underline{h} + x_\theta \underline{h}^t \underline{M}_C \underline{\theta} + \underline{\theta}^t \underline{M}_T \underline{\theta} \right]$$
$$+ \frac{1}{2} \left[\underline{h}^t \underline{K}_B \underline{h} + x_\theta \underline{\theta}^t \underline{K}_C^t \underline{h} + x_\theta \underline{h}^t \underline{K}_C \underline{\theta} + \underline{\theta}^t \underline{K}_T \underline{\theta} \right] \qquad \text{(B2)}$$

For the displacement vectors $\underline{h}$ and $\underline{\theta}$ one can assume expressions of the following form:

$$-\omega_{B_i}^2 \underline{M}_B \underline{h}_i + \underline{K}_B \underline{h}_i = [0] \qquad \underline{h} = a_i \underline{h}_i \qquad \text{(B3)}$$

$$-\omega_{T_j}^2 \underline{M}_T \underline{\theta}_j + \underline{K}_T \underline{\theta}_j = [0] \qquad \underline{\theta} = b_j \underline{\theta}_j \qquad \text{(B4)}$$

Eq. (B2) can then be written as

$$U = -\frac{1}{2}\omega^2 \left[a_i^2 A_i + 2x_\theta a_i b_j C_{ij} + b_j^2 D_j \right]$$
$$+ \frac{1}{2} \left[a_i^2 \underline{h}_i^t \underline{K}_T \underline{h}_i + 2x_\theta a_i b_j B_{ij} + b_j^2 \underline{\theta}_j^t \underline{K}_T \underline{\theta}_j \right] \qquad \text{(B5)}$$

where

$$A_i = \underline{h}_i^t \underline{M}_B \underline{h}_i, \qquad B_{ij} = \underline{\theta}_j^t \underline{K}_C \underline{h}_i, \qquad \text{(B6)}$$

$$C_{ij} = \underline{\theta}_j^t \underline{M}_C \underline{h}_i, \qquad D_j = \underline{\theta}_j^t \underline{M}_T \underline{\theta}_j \qquad \text{(B7)}$$

An application of the principle of minimum potential energy on Eq. (B5) together with Eqs. (B3) and (B4) leads now to the following system of equations:

$$\left[\omega_{B_i}^2 - \omega^2 \right] a_i A_i + x_\theta b_j \left[B_{ij} - \omega^2 C_{ij} \right] = 0 \qquad \text{(B8)}$$

$$\left[\omega_{T_j}^2 - \omega^2 \right] b_j D_j + x_\theta a_i \left[B_{ij} - \omega^2 C_{ij} \right] = 0 \qquad \text{(B9)}$$

Eqs. (B8) and (B9) can be written in matrix form as follows:

$$\begin{bmatrix} (\omega_{B_1}^2-\omega^2)A_1 & & & x_\theta(B_{11}-\omega^2C_{11}) & & \\ & (\omega_{B_2}^2-\omega^2)A_2 & & x_\theta(B_{21}-\omega^2C_{21}) & & \\ & & \ddots & \vdots & & \\ & & & & & \\ x_\theta(B_{11}-\omega^2C_{11}) & & & (\omega_{T_1}^2-\omega^2)D_1 & & \\ x_\theta(B_{12}-\omega^2C_{12}) & & & & (\omega_{T_2}^2-\omega^2)D_2 & \\ & & & & & \ddots \end{bmatrix} \begin{bmatrix} a_1 \\ a_2 \\ \vdots \\ a_m \\ b_1 \\ b_2 \\ \vdots \\ b_n \end{bmatrix} = \begin{bmatrix} 0 \\ 0 \\ \vdots \\ 0 \\ 0 \\ 0 \\ \vdots \\ 0 \end{bmatrix} \qquad \text{(B10)}$$

The terms $\omega_{B_i}^2$, $\omega_{T_j}^2$, A_i, B_{ij}, C_{ij}, and D_j in Eq. (B10) can be evaluated for an uncoupled system of equations. Eq. (B10) can then be solved to obtain coupled frequencies.

The stability of Eqs. (B8) and (B9) can be tested by determining whether or not the mass matrix is positive definite. In matrix notation this can be shown as

$$\det \begin{bmatrix} A_1 & & & x_\theta C_{11} & x_\theta C_{12} & \cdot & \cdot \\ & A_2 & & x_\theta C_{21} & & & \\ & & \cdot & \cdot & & & \\ & & & \cdot & & & \\ x_\theta C_{11} & x_\theta C_{21} & \cdot \; \cdot & D_1 & & & \\ x_\theta C_{12} & & & & D_2 & & \\ \cdot & & & & & \cdot & \\ \cdot & & & & & & \cdot \end{bmatrix} = 0 \qquad \text{(B11)}$$

APPENDIX C

FINITE ELEMENT FORMULATION OF MASS AND STIFFNESS MATRICES FOR THE COUPLED EQUATIONS OF MOTION

The finite element method was used for a discretized representation of the mass and stiffness properties of the rotor blade. The coupled equations of motion (Eqs. (7) and (8)) were written as a system of matrix differential equations. To analyze the torsional vibrations, a constant strain element was used which requires a linear variation of displacement over the element, while for bending vibrations a quadratic displacement function was employed.

Formulation of Mass and Stiffness Matrices for Torsional Vibrations

A consistent mass matrix was used for the discretized representation of the inertia term in the equation of motion (A1). The derivation of the mass matrix for torsional vibrations will now be summarized. For the blade element in figure 18, with nodal torsional rotations θ_1 and θ_2, the rotation at any point can be expressed as

$$\theta = [1-\zeta \quad \zeta] \begin{bmatrix} \theta_1 \\ \theta_2 \end{bmatrix} \tag{C1}$$

The torsional acceleration at any point can then be written as

$$\frac{d^2\theta}{dt^2} = [1-\zeta \quad \zeta] \begin{bmatrix} \frac{d^2\theta_1}{dt^2} \\ \frac{d^2\theta_2}{dt^2} \end{bmatrix} \tag{C2}$$

The equivalent inertia forces at the nodes of a blade finite element can be defined as a vector $\underline{T}$ using the principle of virtual work as follows:

$$\underline{\theta}^t \underline{T} = \underline{\theta}^t \int_0^{\ell} I_\theta \begin{bmatrix} 1-\zeta \\ \zeta \end{bmatrix} [1-\zeta \quad \zeta] \, dx \, \ddot{\underline{\theta}} \tag{C3}$$

or

$$\underline{T} = \frac{I_\theta \ell}{6} \begin{bmatrix} 2 & 1 \\ 1 & 2 \end{bmatrix} \begin{bmatrix} \frac{d^2\theta_1}{dt^2} \\ \frac{d^2\theta_2}{dt^2} \end{bmatrix} \tag{C4}$$

The elemental torsional mass matrix can be written as

$$\underline{M}_{T_i} = \frac{I_\theta \ell}{6} \begin{bmatrix} 2 & 1 \\ 1 & 2 \end{bmatrix} \tag{C5}$$

The elemental stiffness matrix can be analyzed in two parts. The first part is the elastic stiffness matrix, while the second part is the matrix representing the effect of the centrifugal forces along the blade axis. For a linear variation of torsional displacements over a finite element, using an approach similar to the derivation of the mass matrix, the effect of the centrifugal forces can be represented by a geometric stiffness matrix. The torsional stiffness matrix for a rotating blade element can then be written as

$$\underline{K}_{T_i} = \frac{JG}{\ell} \begin{bmatrix} 1 & -1 \\ -1 & 1 \end{bmatrix} + \Omega^2 \frac{I_\theta \ell}{6} \begin{bmatrix} 2 & 1 \\ 1 & 2 \end{bmatrix} \tag{C6}$$

Formulation of the Mass and Stiffness Matrices for Bending Vibrations

After defining the nodal force vector $\underline{P}$ and the nodal displacement vector $\underline{\rho}$, as shown in figure 18, the vertical displacement, h, at any point can be expressed in terms of the nodal displacements as follows:

$$h = \begin{bmatrix} (1 - 3\zeta^2 + 2\zeta^3) & \ell(\zeta - 2\zeta^2 + \zeta^3) & (3\zeta^2 - 2\zeta^3) & \ell(-\zeta^2 + \zeta^3) \end{bmatrix} \begin{bmatrix} \rho_1 \\ \rho_2 \\ \rho_3 \\ \rho_4 \end{bmatrix} \tag{C7}$$

A consistent mass matrix can also be derived for the bending vibrations of the finite element using the approach applied for torsional vibrations. Neglecting the effect of the shear deformations, the mass matrix in bending can be written as

$$\underline{M}_{B_i} = \frac{m\ell}{420}\begin{bmatrix} 156 & & & \\ 22\ell & 4\ell^2 & \text{Symmetric} & \\ 54 & 13\ell & 156 & \\ -13\ell & -3\ell^2 & -22\ell & 4\ell^2 \end{bmatrix} \tag{C8}$$

In the case of a rotating blade the bending stiffness can also be analyzed in two parts as elastic stiffness and geometric stiffness due to the axial forces in the blade. The representation of the elastic stiffness of a blade element is well known [5]. The effect of rotation of the blade can be evaluated by making use of a geometric stiffness matrix, which has already been used for solving stability problems [5].

From Eq. (A1), the following relationship can be written for the finite element to represent the virtual work by axial forces:

$$\underline{\rho}^t \underline{P} = \int_0^{\ell} h' \, Th' \, dx \tag{C9}$$

Substituting Eq. (C7) into Eq. (C9), the bending stiffness of the blade element due to axial forces can be calculated. The total stiffness matrix in bending can then be written as

$$\underline{K}_{B_i} = \begin{bmatrix} \frac{12EI}{\ell^3} & & & \\ \frac{6EI}{\ell^2} & \frac{4EI}{\ell} & \text{Symmetric} & \\ \frac{-12EI}{\ell^3} & \frac{-6EI}{\ell^2} & \frac{12EI}{\ell^3} & \\ \frac{6EI}{\ell^2} & \frac{2EI}{\ell} & \frac{-6EI}{\ell^2} & \frac{4EI}{\ell} \end{bmatrix} + \frac{T}{\ell}\begin{bmatrix} \frac{6}{5} & & & \\ \frac{\ell}{10} & \frac{2\ell^2}{15} & \text{Symmetric} & \\ \frac{-6}{5} & \frac{-\ell}{10} & \frac{6}{5} & \\ \frac{\ell}{10} & \frac{-\ell^2}{30} & \frac{-\ell}{10} & \frac{2\ell^2}{15} \end{bmatrix} \tag{C10}$$

The displacement functions were defined for a blade element in bending, Eq. (C7), and for torsion, Eq. (C1). Using the principle of virtual work, the coupling terms in Eqs. (7) and (8) can be derived for the defined displacement functions.

Derivation of the Coupled Mass Term ($mx_\theta\ddot{\theta}$)

The virtual work due to the coupled mass term can be expressed as

$$\underline{\rho}^t\,\underline{P} = \int_o^\ell h\,m\,x_\theta\ddot{\theta}\,dx \tag{C11}$$

Substituting Eqs. (C2) and (C7) into Eq. (C11) one can obtain Eq. (C12).

$$\underline{P} = \frac{m\,x_\theta\,\ell}{60}\begin{bmatrix} 21 & 9 \\ 3\ell & 2\ell \\ 9 & 21 \\ -2\ell & -3\ell \end{bmatrix}\begin{bmatrix} \ddot{\theta}_1 \\ \ddot{\theta}_2 \end{bmatrix} \tag{C12}$$

Derivation of the Coupled Stiffness Term $(\Omega^2\,mr\,x_\theta)'$

The virtual work due to this term can be formulated as

$$\underline{\rho}^t\,\underline{P} = \int_o^\ell \Omega^2\,mr\,x_\theta\,\theta h'\,dx \tag{C13}$$

Assuming that the length of the finite element is small in comparison to r, Eqs. (C1), (C7), and (C13) yield the following expression:

$$\underline{P} = \frac{\Omega^2\,mr\,x_\theta}{12}\begin{bmatrix} -6 & -6 \\ \ell & -\ell \\ 6 & 6 \\ -\ell & \ell \end{bmatrix}\begin{bmatrix} \theta_1 \\ \theta_2 \end{bmatrix} \tag{C14}$$

Determination of the Coupled Mass and Stiffness Matrices

Mass and stiffness matrices in bending and torsion can be combined to obtain a single mass-stiffness representation of the finite element for describing the coupled behavior. Combining the mass and stiffness matrices from Eqs. (C5), (C6), (C8), (C10), (C12), and (C14), and defining the force and displacement vectors for the element as

$$\underline{P} = \begin{bmatrix} P_1 \\ P_2 \\ T_1 \\ P_3 \\ P_4 \\ T_2 \end{bmatrix} \qquad \underline{\rho} = \begin{bmatrix} \rho_1 \\ \rho_2 \\ \theta_1 \\ \rho_3 \\ \rho_4 \\ \theta_2 \end{bmatrix} \tag{C15}$$

the coupled mass and stiffness matrices for the element can be written as

$$\underline{M}_i = \frac{m\ell}{420} \begin{bmatrix} 156 & & & & & \\ 22\ell & 4\ell^2 & & & \text{Symmetric} & \\ 147x_\theta & 21\ell x_\theta & 140(I_\theta/m+x_\theta^2) & & & \\ 54 & 13\ell & 63x_\theta & 156 & & \\ -13\ell & -3\ell^2 & -14\ell x_\theta & -22\ell & 4\ell^2 & \\ 63x_\theta & 14\ell x_\theta & 70(I_\theta/m+x_\theta^2) & 147x_\theta & -21\ell x_\theta & 140(I_\theta/m+x_\theta^2) \end{bmatrix} \tag{C16}$$

$$
\underline{K}_i = \begin{bmatrix}
\frac{12EI}{\ell^3} + \frac{6T}{5\ell} & & & & & & & & & \\
\frac{6EI}{\ell^2} + \frac{T}{10} & \frac{4EI}{\ell} + \frac{2T\ell}{15} & & & & & & & & \\
-\frac{\Omega^2 m r x_\theta}{2} & \frac{\Omega^2 m r x_\theta \ell}{12} & \frac{\Omega^2 I_\theta \ell}{3} + \frac{(GJ+Tx_\theta^2)}{\ell} & & & & & \text{Symmetric} & & \\
-\frac{12EI}{\ell^3} - \frac{6T}{5\ell} & -\frac{6EI}{\ell^2} - \frac{T}{10} & \frac{\Omega^2 m r x_\theta}{2} & \frac{12EI}{\ell^3} + \frac{6T}{5\ell} & & & & & & \\
\frac{6EI}{\ell^2} + \frac{T}{10} & \frac{2EI}{\ell} - \frac{T\ell}{30} & -\frac{\Omega^2 m r x_\theta \ell}{12} & -\frac{6EI}{\ell^2} - \frac{T}{10} & \frac{4EI}{\ell} + \frac{2\ell T}{15} & & & & & \\
-\frac{\Omega^2 m r x_\theta}{2} & -\frac{\Omega^2 m r x_\theta \ell}{12} & -\frac{(GJ+Tx_\theta^2)}{\ell} + \frac{\Omega^2 I_\theta \ell}{6} & \frac{\Omega^2 m r x_\theta}{2} & \frac{\Omega^2 m r x_\theta \ell}{12} & \frac{(GJ+Tx_\theta^2)}{\ell} + \frac{\Omega^2 I_\theta \ell}{3} & & & &
\end{bmatrix}
\tag{C17}
$$

REFERENCES

1. Houbolt, J. C., and Brooks, G.W.: Differential Equations of Motion for Combined Flapwise Bending, Chordwise Bending, and Torsion of Twisted Non-Uniform Rotor Blades. NACA Note 3095, 1957.

2. Isakson, G., and Eisley, J. G.: Natural Frequencies in Coupled Bending and Torsion of Twisted Rotating and Nonrotating Blades. NASA CR-65, 1964.

3. Garland, C. F.: The Normal Modes of Vibrations of Beams Having Non-collinear Elastic and Mass Axes. J. of App. Mechs., Sept., 1940.

4. Perisho, C. H.: Analysis of the Stability of a Flexible Rotor Blade at High Advance Ratio. J. of Am. Helicopter Soc., Vol. 13, No. 3, 1968.

5. Przemieniecki, J. S.: Theory of Matrix Structural Analysis. McGraw-Hill Book Co., New York, 1968.

TABLE 1. CH-34 Blade Physical Properties:

Length of the blade = 8.534 m.

Elastic tensile modulus = 7.0308×10^{9} Kg./m^2

Normal rotor speed - 23.1 rad./sec.

Blade chord - .416 m.

RADIAL LOCATION	ELEMENT LENGTH (m.)	WEIGHT PER UNIT LENGTH (Kg./m.)	FLAPWISE AREA MOMENT (m^4)	TORSIONAL INERTIA (Kg.-sec^2)	TORSIONAL RIDIGITY (kg.-m^2)
Tip	.406	14.286	4.203×10^{-7}	9.5×10^{-3}	5.267×10^{3}
	.508	9.822	6.035	7.7	5.267
	.508	10.714	6.035	8.6	5.267
	.508	9.107	6.035	7.3	5.267
	.508	9.822	6.035	7.7	5.267
	.508	8.929	6.118	7.3	5.267
	.508	8.929	6.118	7.3	5.267
	.508	9.018	6.118	7.5	5.267
	.508	9.643	6.035	7.5	5.267
	.508	8.929	6.118	7.3	5.267
	.508	9.643	6.035	7.5	5.267
	.508	8.929	6.118	7.3	5.267
	.508	9.286	6.035	7.4	5.267
	.508	7.143	6.909	5.9	5.852
	.508	6.250	7.700	3.6	6.437
	.508	4.053	116.128	27.2	7.227
Hinge	.203	160.724	86.576	66.7	32.74
	.304	357.165	332.985	453.6	146.30

TABLE 2. Uncoupled Frequencies of CH-34 Blade in Bending and Torsion:

Mode No.	Bending (rad/sec.)	Torsion (rad/sec.)
1	25.2	173.6
2	72.4	532.1
3	136.2	934.9
4	210.8	1350.0

TABLE 3. The Frequencies Corresponding to the Coupled Modes, Consisting Mainly of First Mode in Bending and First Mode in Torsion.

x_θ (m)	ω_B^2 (rad^2/sec.^{2})	ω_T^2 (rad^2/sec.^{2})
0.0	635.0	30,137
0.020	632.8	31,959
.041	626.2	38,499
.050	622.4	47,284
.060	616.3	59,349
.069	611.0	83,710
.077	604.9	146,223
.083	600.5	289,632
.104	581.9	-71,923
.124	559.6	-31,572
.145	539.0	-18,779
.187	473.7	-9,520

TABLE 4a. Generalized Structural Mass ($\alpha_{ij} = \underline{p}_i^t \underline{M} \underline{p}_j$), x_θ = .0254 m for Uncoupled Modes of CH-34 Blade

		Bending Modes			Torsional Modes		
		1	2	3	1	2	3
		Kg. $sec.^2/m.$			Kg. $sec.^2$		
Bending Modes	1.	3.0160	0.0000	0.0000	0.8399	$-.1784 \times 10^{-2}$	$-.2592 \times 10^{-2}$
	2.	0.0000	1.9366	0.0000	$-.3127 \times 10^{-2}$	-.0640	$.8074 \times 10^{-2}$
	3.	0.0000	0.0000	1.8445	$.3221 \times 10^{-2}$	$.8977 \times 10^{-2}$	.0604
		Kg. $sec.^2$			Kg. $sec.^2$ m.		
Torsional Modes	1.	0.0839	$-.3127 \times 10^{-2}$	$.3221 \times 10^{-2}$	$.2817 \times 10^{-1}$	0.0000	0.0000
	2.	$-.1784 \times 10^{-2}$	-.0640	$.8977 \times 10^{-2}$	0.0000	$.2668 \times 10^{-1}$	0.0000
	3.	$-.2592 \times 10^{-2}$	$.8074 \times 10^{-1}$	.0604	0.0000	0.0000	$.2579 \times 10^{-1}$

TABLE 4b. Generalized Structural Stiffness ($\gamma_{ij} = \underline{p}_i^t \underline{K} \underline{p}_j$), x_θ = .0254 m. for Uncoupled Modes of CH-34 Blade

		Bending Modes			Torsional Modes		
		1	2	3	1	2	3
		Kg/m.			Kg.		
Bending Modes	1.	1.8058×10^3	0.0000	0.0000	$-.4378 \times 10^2$	$-.1449 \times 10^3$	$-.1407 \times 10^3$
	2.	0.0000	8.4362×10^3	0.0000	$-.2636 \times 10^1$	$.7629 \times 10^2$	$.1960 \times 10^3$
	3.	0.0000	0.0000	2.6117	$-.0763 \times 10^1$	$.3531 \times 10^1$	$-.1082 \times 10^3$
		Kg.			Kg. m.		
Torsional Modes	1.	$-.4378 \times 10^2$	$-.2636 \times 10^1$	$-.0763 \times 10^1$	8.4207×10^2	0.0000	0.0000
	2.	$-.1449 \times 10^3$	$.7629 \times 10^2$	$.3532 \times 10^1$	0.0000	7.2324×10^3	0.0000
	3.	$-.1407 \times 10^3$	$.1960 \times 10^3$	$-.1082 \times 10^3$	0.0000	0.0000	2.0219×10^4

TABLE 5. Uncoupled Generalized Structural Mass (α_i), Critical Damping (β_i), and Stiffness (γ_i) of CH-34 Blade

	Bending Modes			Torsional Modes		
	1	2	3	1	2	3
	(Kg. sec.^{2}/m.)			(Kg. sec.^{2}/m.)		
α_i	3.0160	1.9306	1.8445	4.4356×10^2	4.2012×10^2	4.0622×10^2
	(Kg. sec./m.)			(Kg. sec./m.)		
β_i	1.4759×10^2	2.5524×10^2	4.3898×10^2	1.5339×10^4	4.3750×10^4	7.1936×10^4
	(Kg./m.)			(Kg./m.)		
γ_i	1.8058×10^1	8.4362×10^3	2.6117×10^4	1.3261×10^6	1.1389×10^5	3.1848×10^7

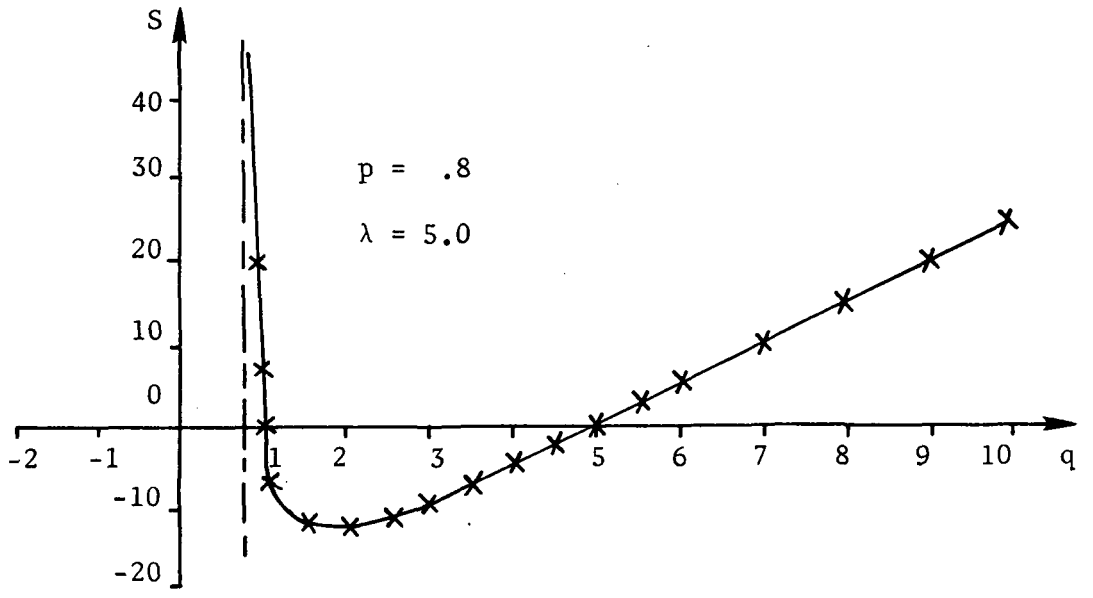

Fig. 1 Variation of Coupled Frequencies of Rotating Blades Using:

$$S_1 = \frac{(1-q)\ (\lambda-q)}{(p-q)\ (p-1)}$$

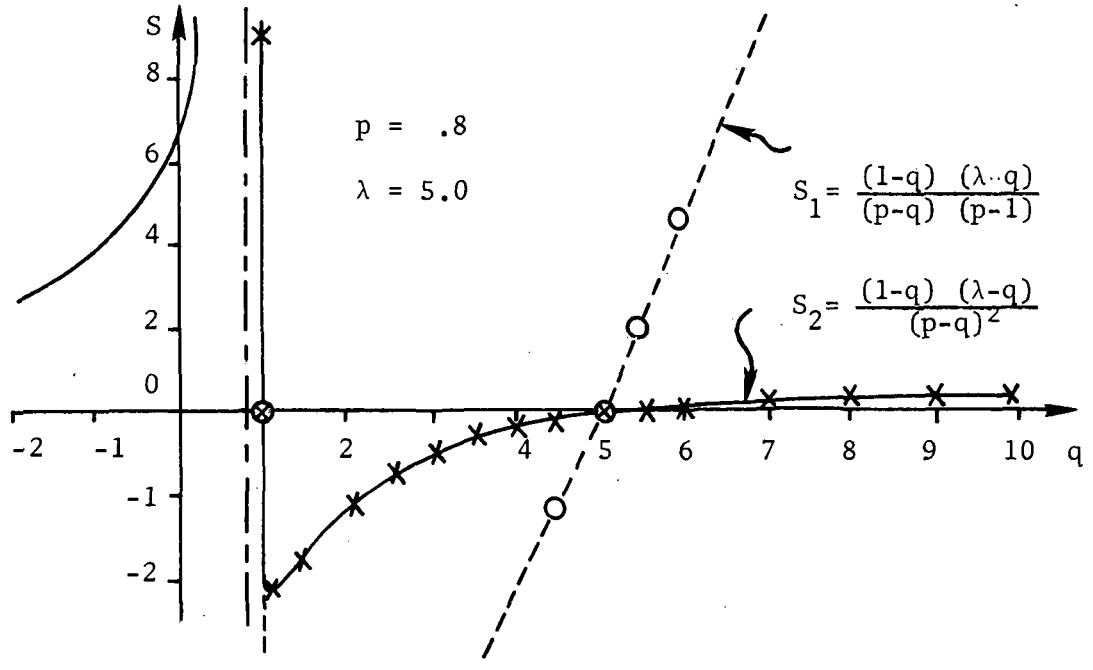

Fig. 2 Variation of Coupled Frequencies of Rotating Blades Using:

$$S_2 = \frac{(1-q)\ (\lambda-q)}{(p-q)^2}$$

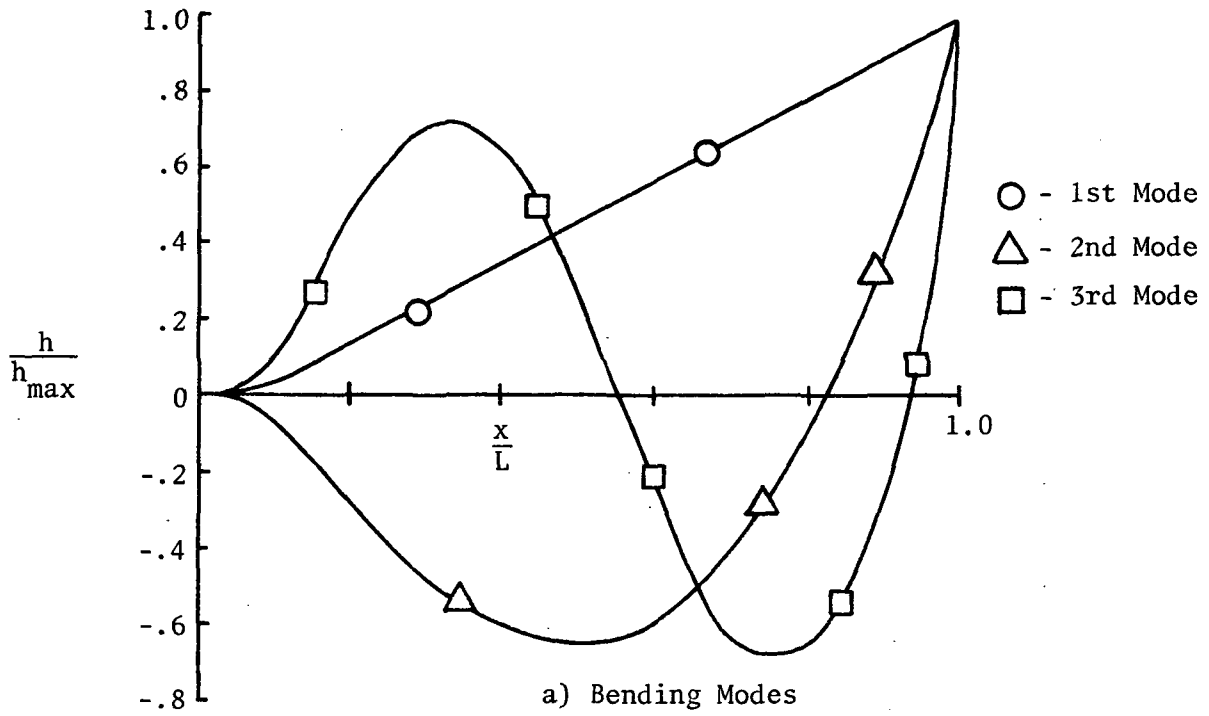

a) Bending Modes

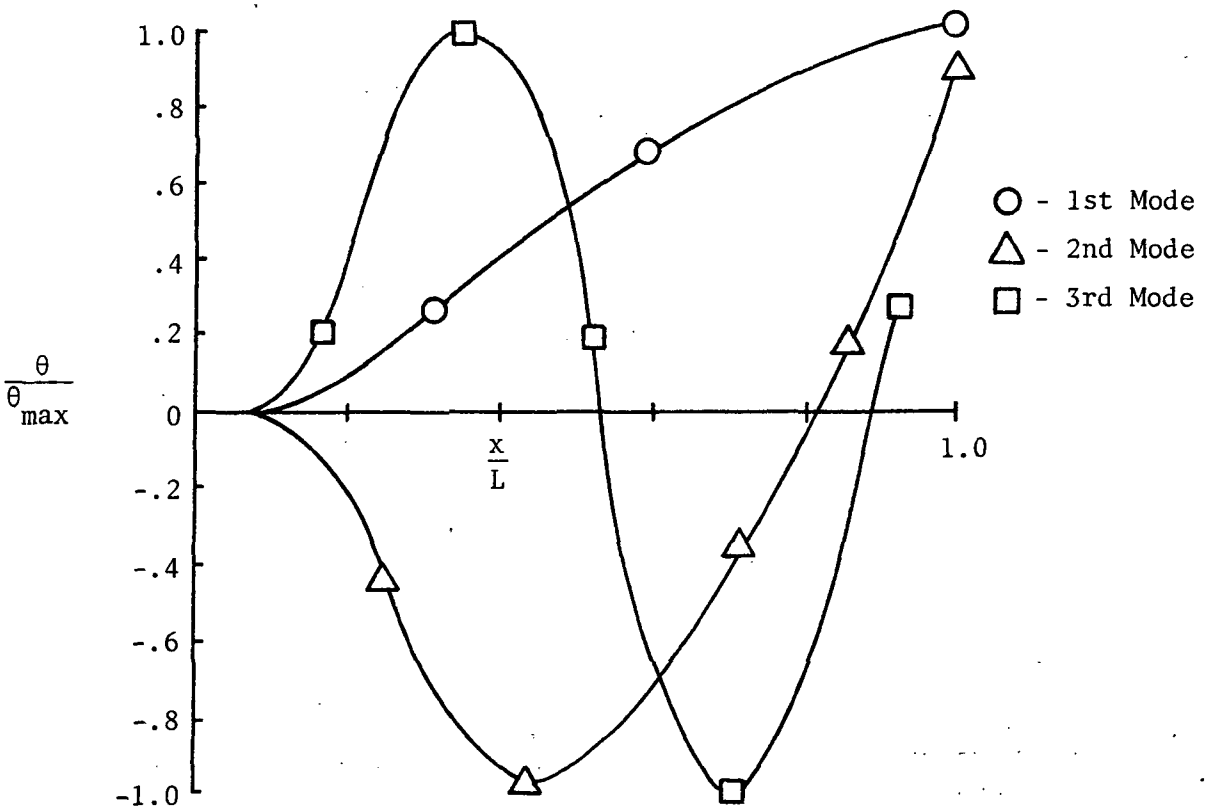

b) Torsional Modes

Fig. 3 Uncoupled Natural Vibration Modes of CH-34 Blade.

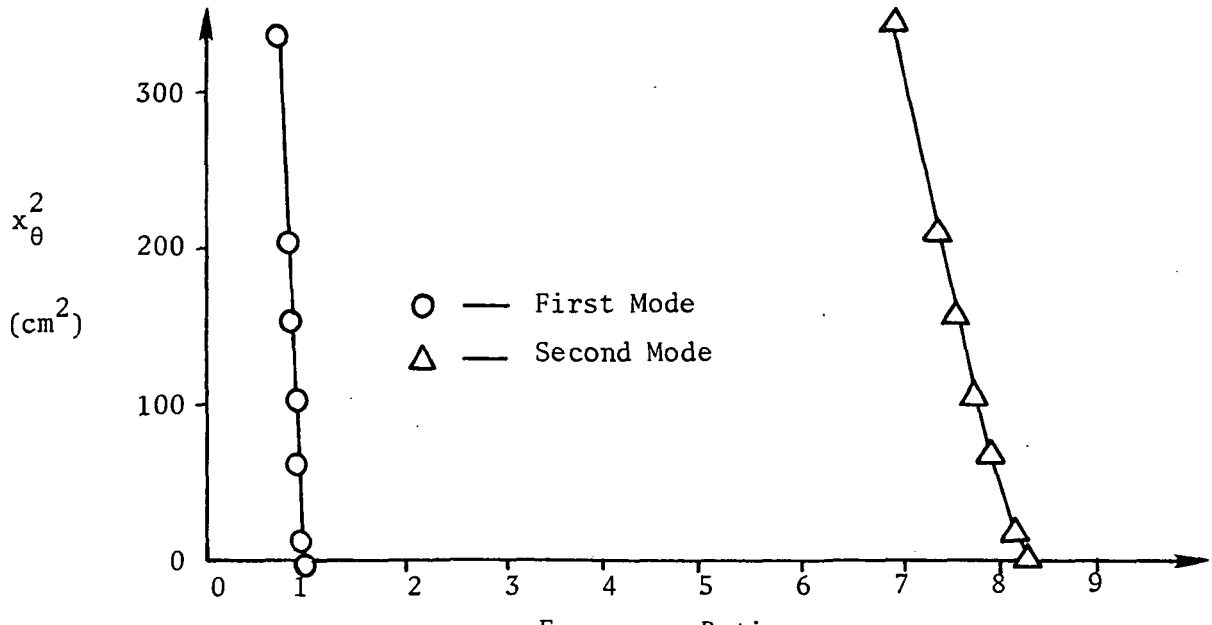

Fig. 4 Variation of the Two Lowest Frequencies Corresponding to a Mainly Bending Mode with Increasing Eccentricity.

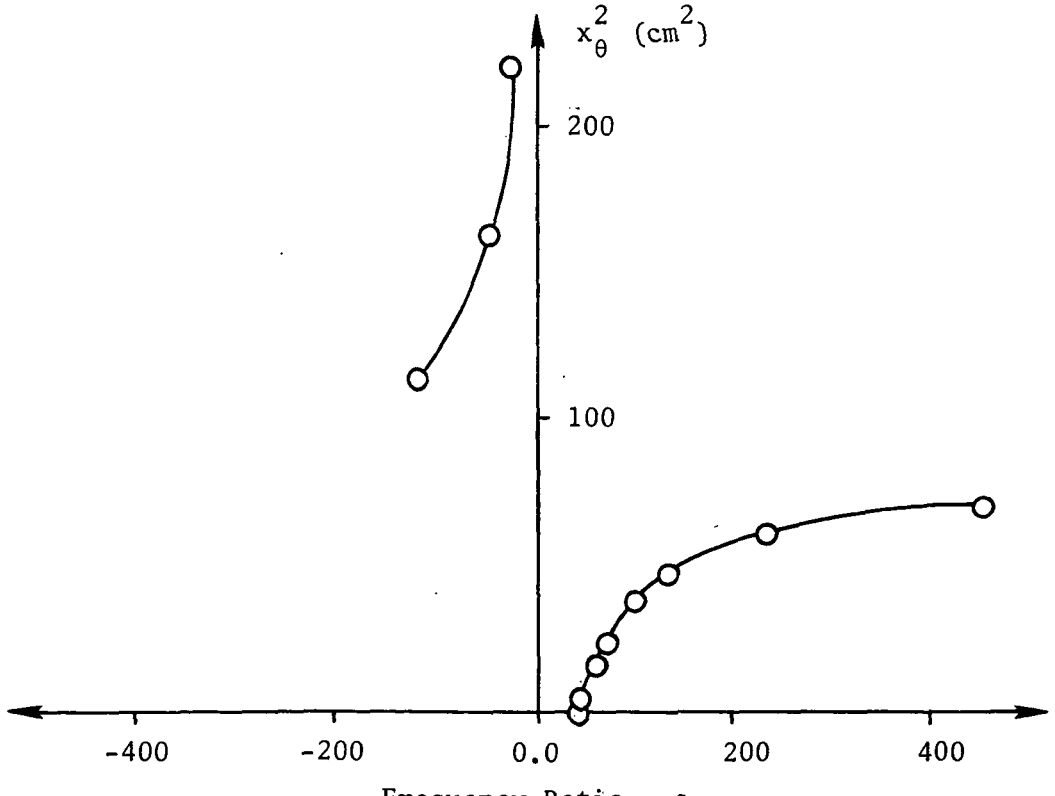

Fig. 5 Variation of the Lowest Frequency Corresponding to a Mainly Torsional Mode with Increasing Eccentricity.

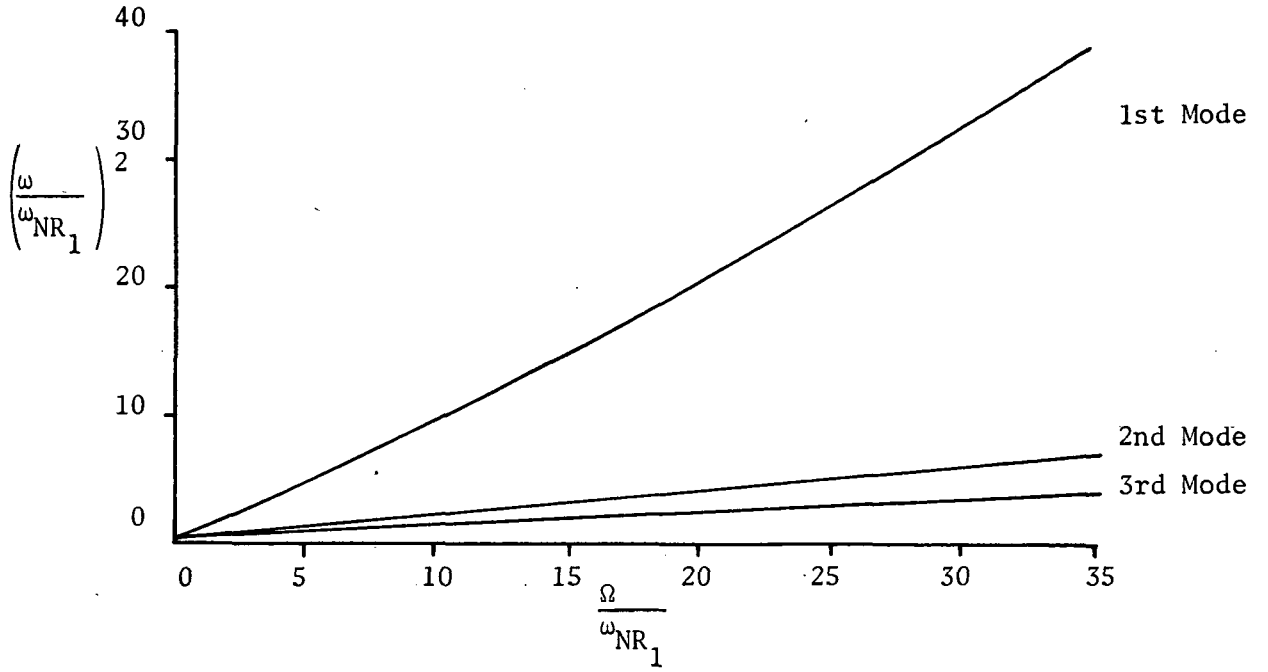

Fig. 6 Variation of Lowest Bending Frequencies for a Hinged Blade (CH-34) with Blade Rotational Velocity, (x_θ = 0.0 and 3.28).

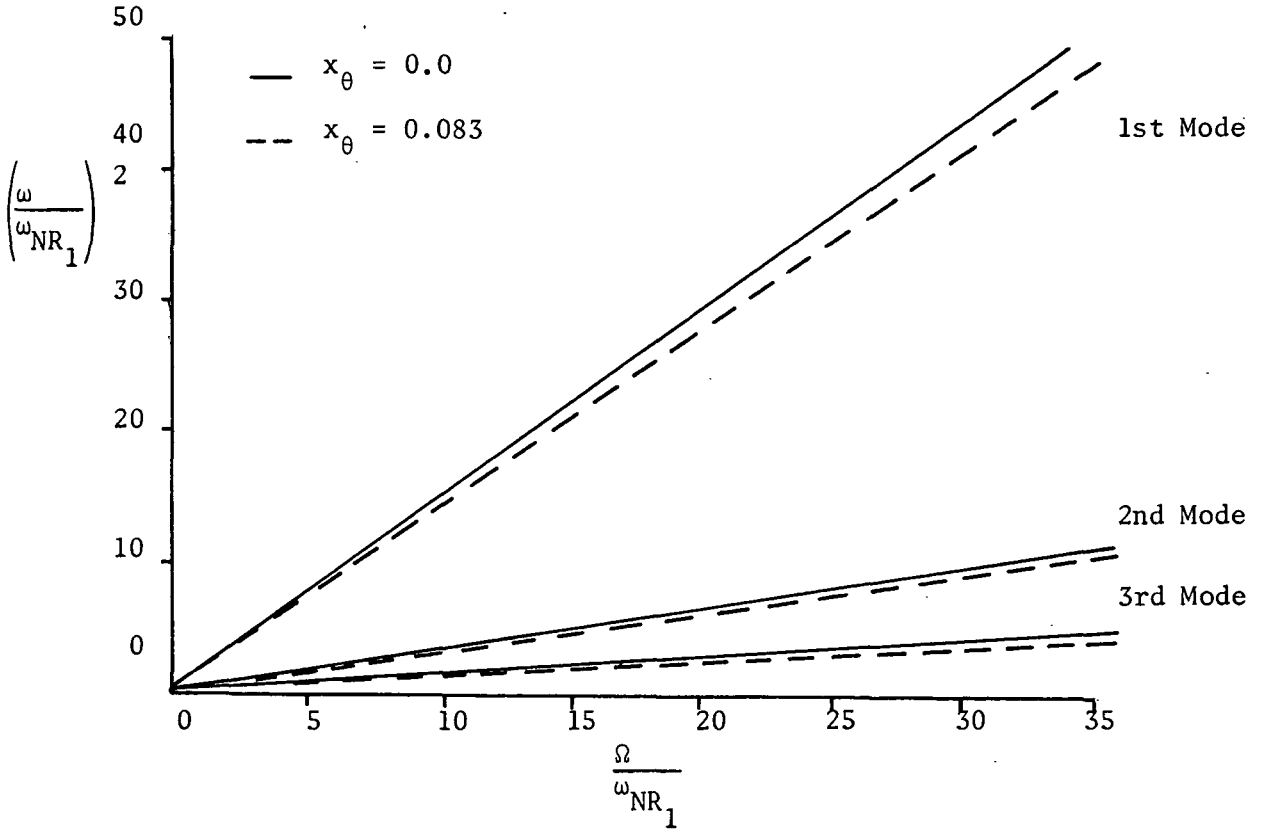

Fig. 7 Variation of Lowest Bending Frequencies for a Cantilever Blade (CH-34) with Blade Rotational Velocity.

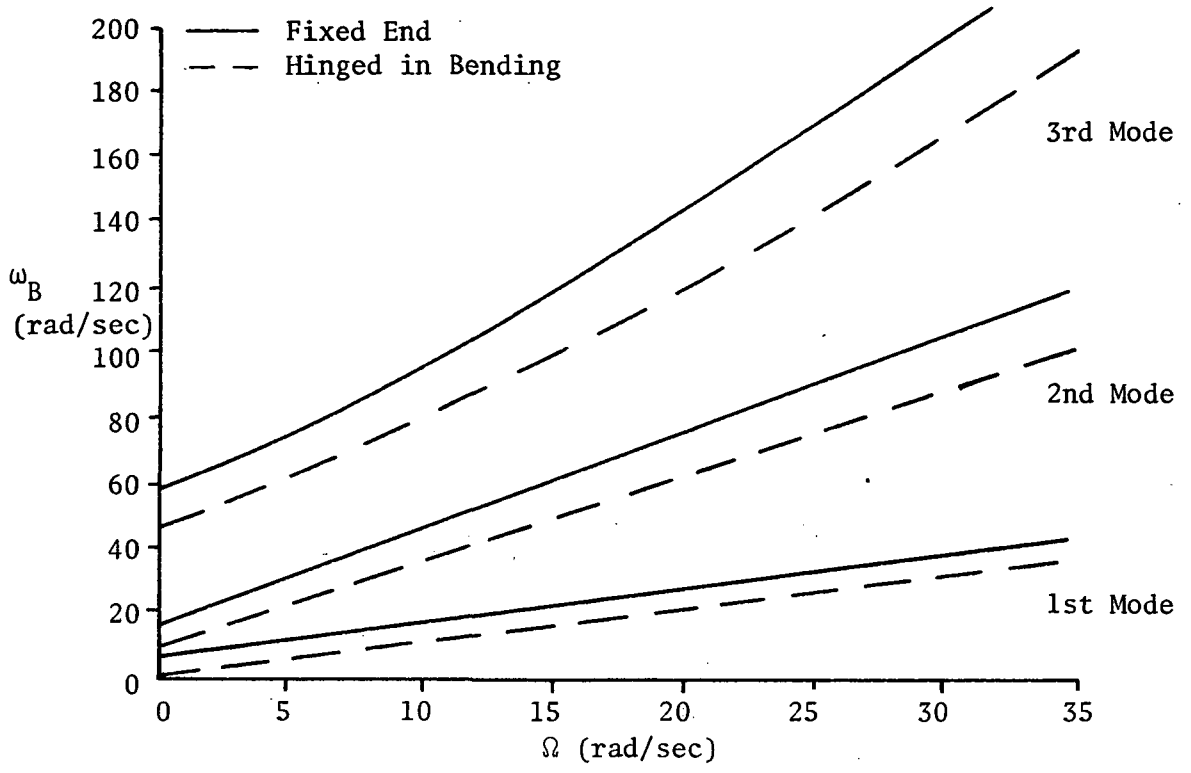

Fig. 8 Variation of Lowest Bending Frequencies for a Cantilever and Hinged Blade (CH-34) with Blade Rotational Velocity.

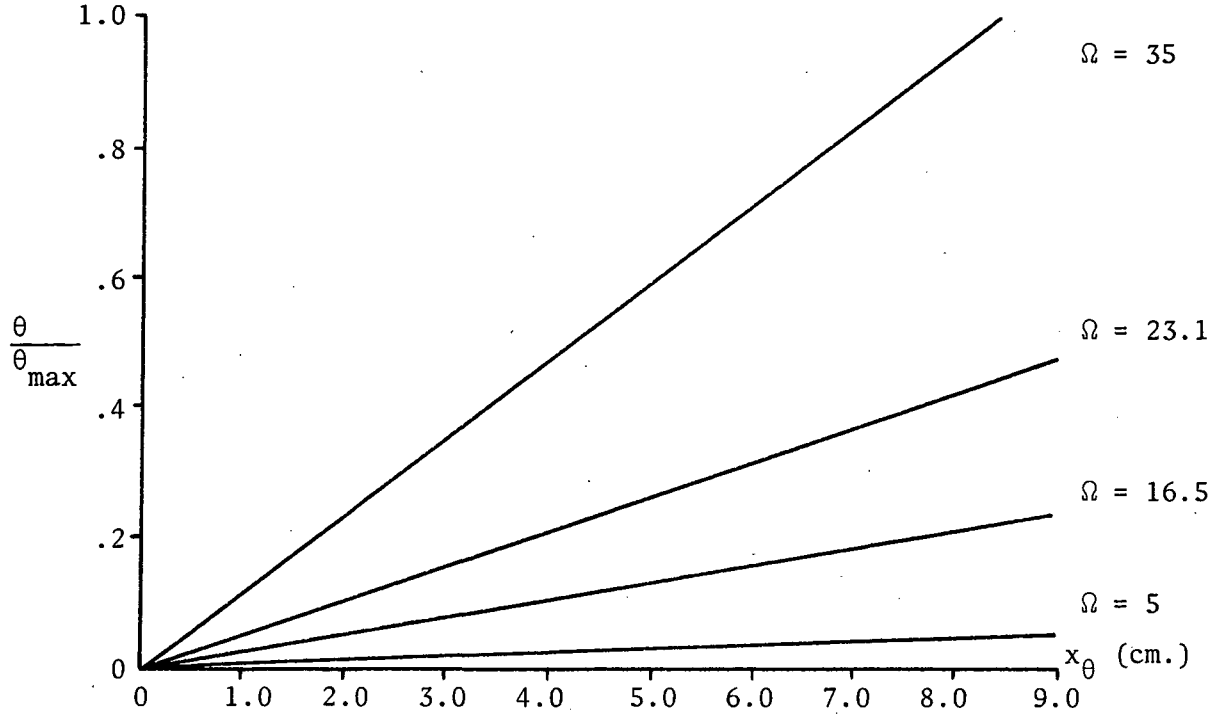

Fig. 9 Variation of the Torsional Rotations at the Blade Tip with Eccentricity.

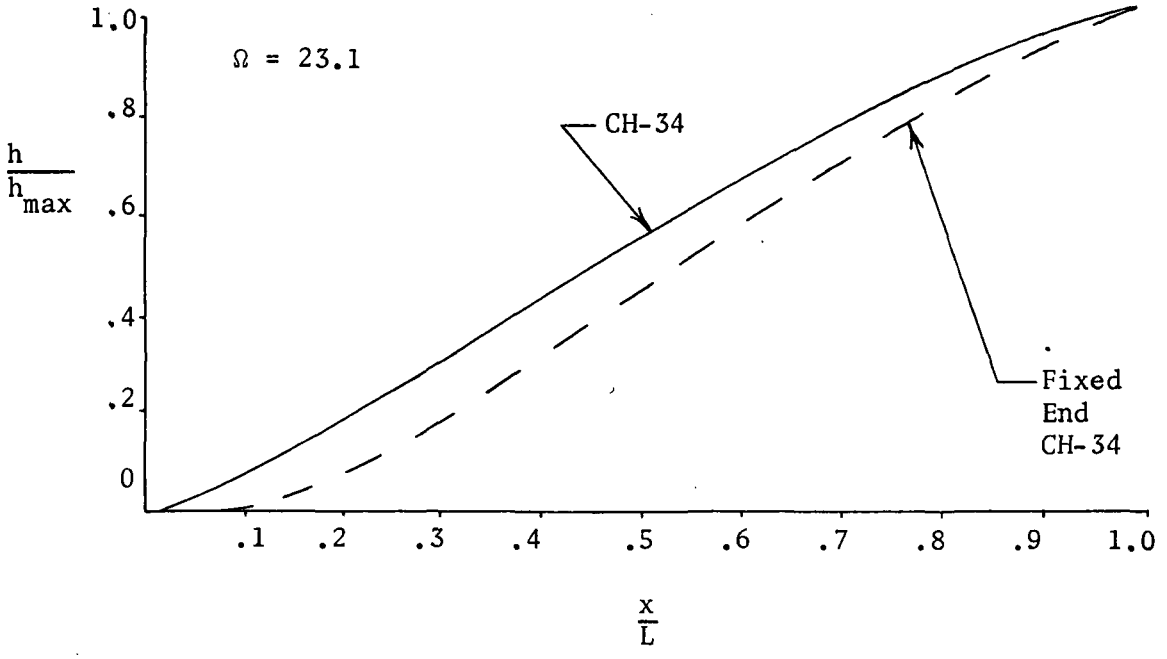

Fig. 10 First Uncoupled Bending Mode for CH-34 and Fixed End CH-34.

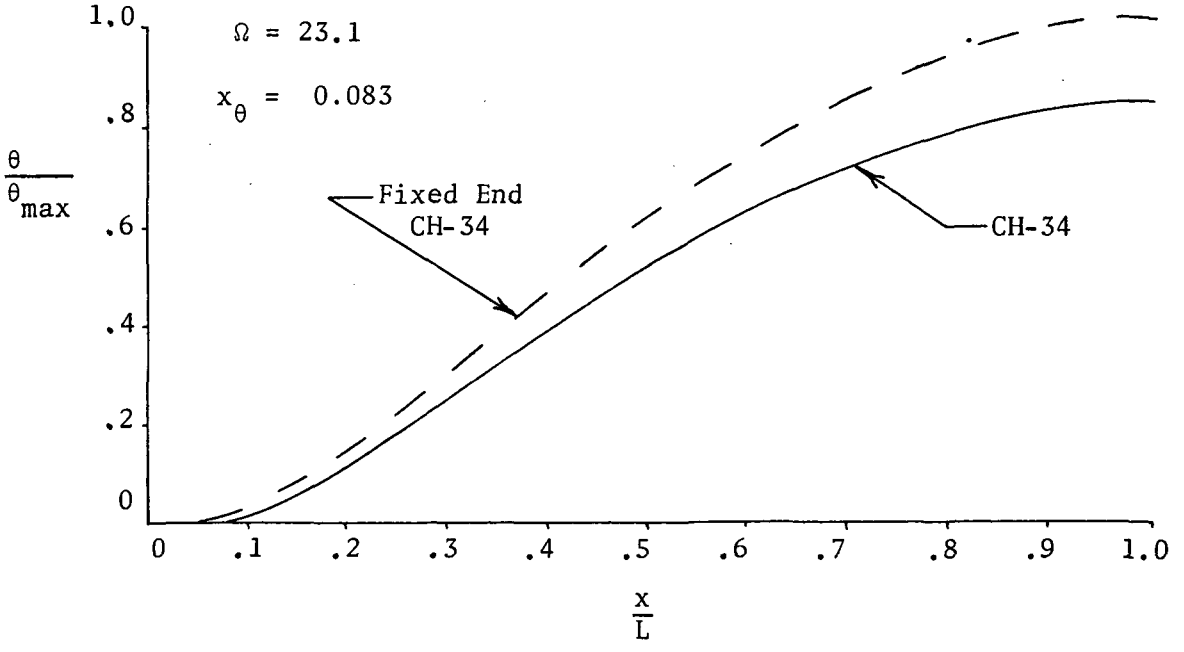

Fig. 11 Torsional Component of First Coupled Mode for CH-34 and Fixed End CH-34.

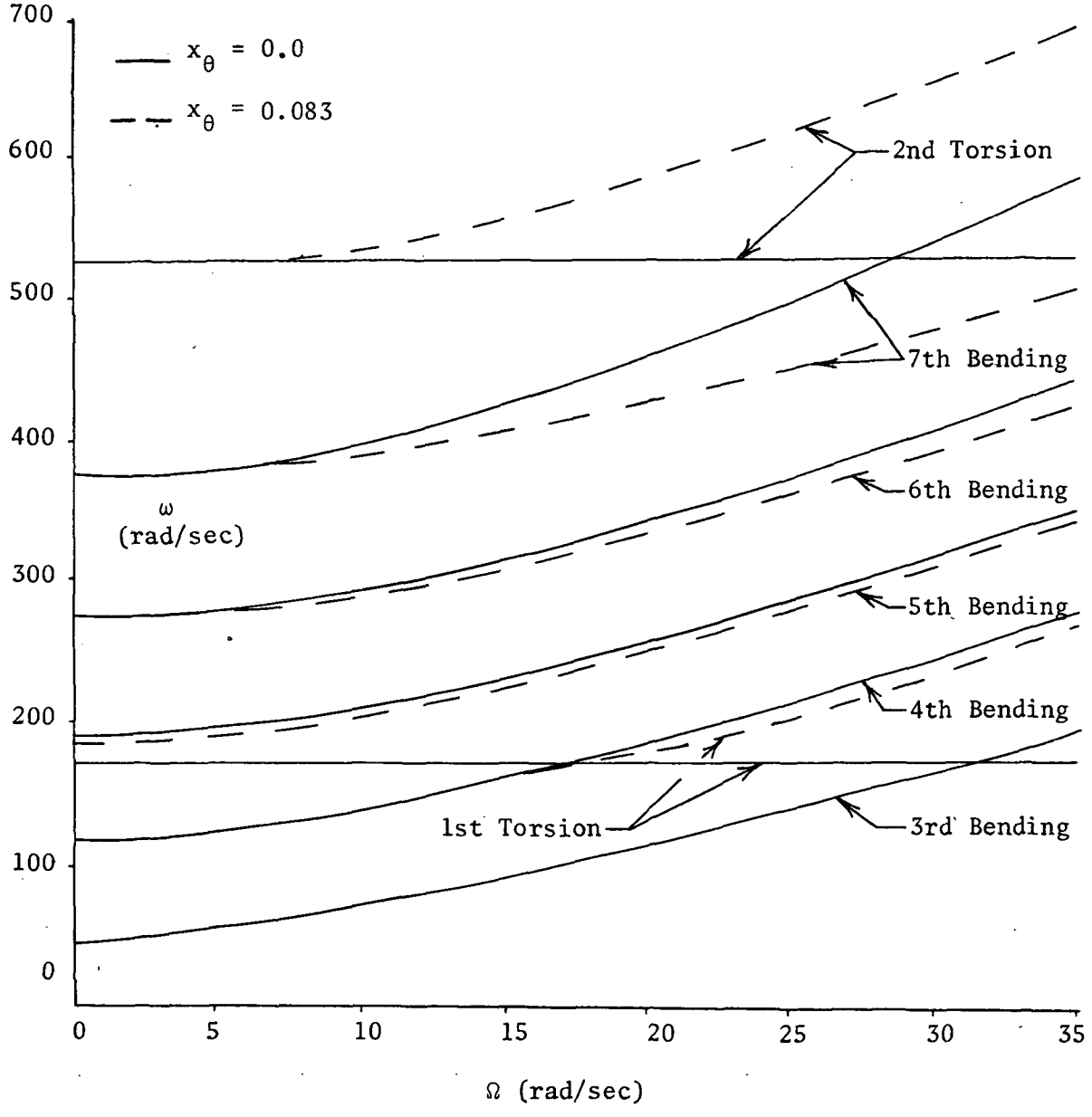

Fig. 12 Interaction Between Mainly Torsional Modes and Higher Bending Modes.

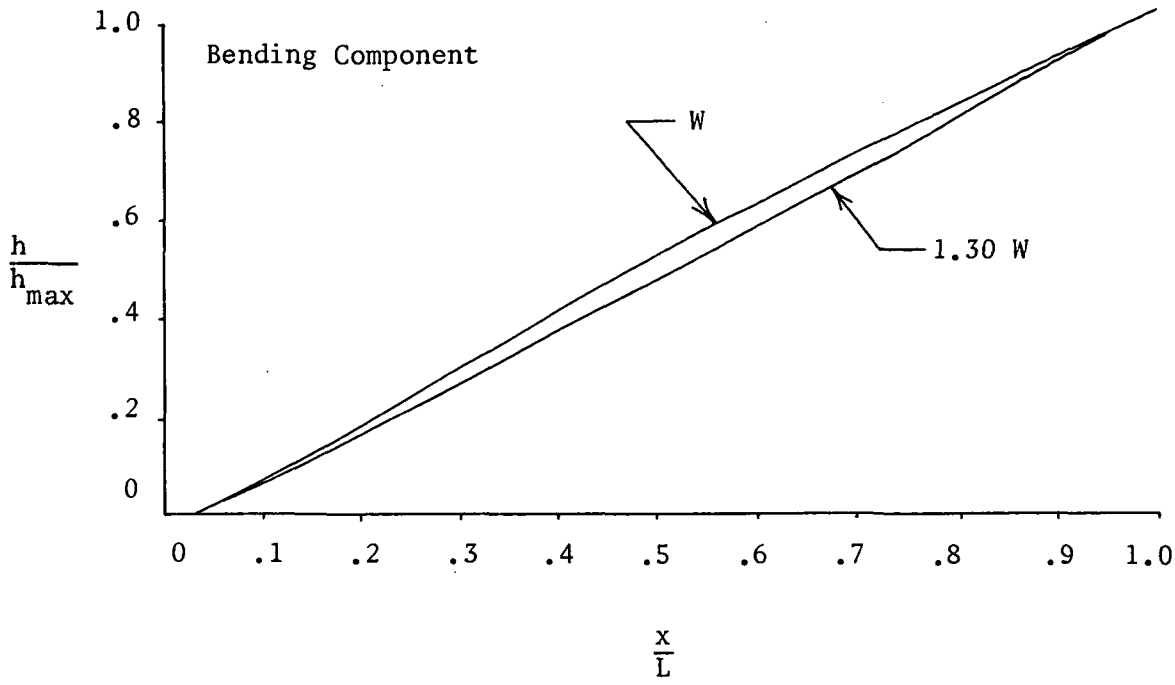

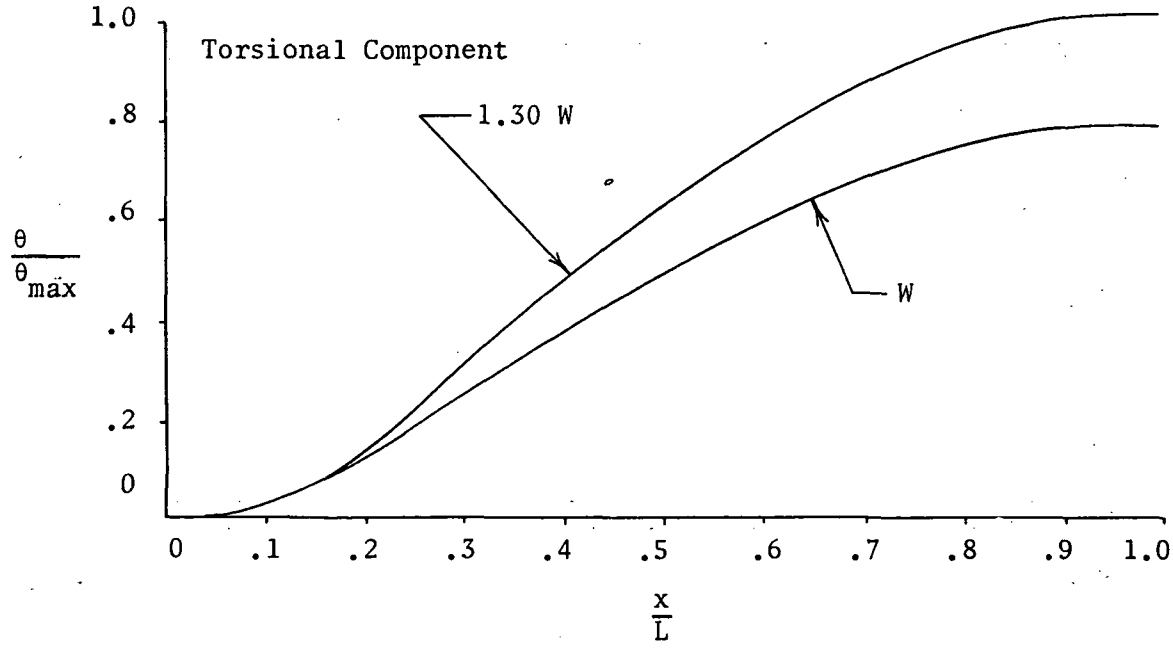

Fig. 13 Variation of First Coupled Modes with 30% Increase in Weight Distribution (W), (CH-34).

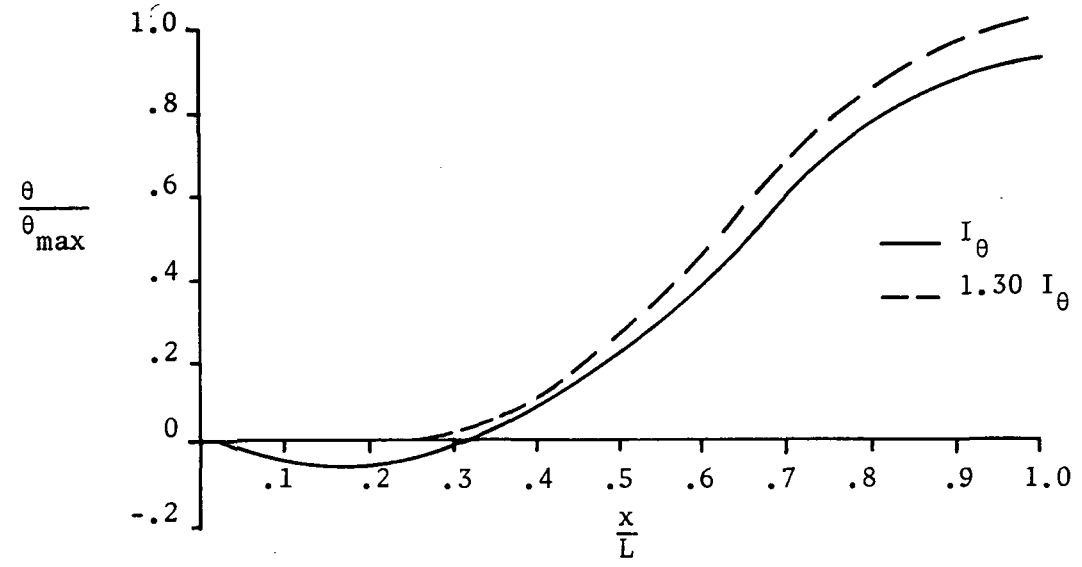

Fig. 14 Variation of Second Coupled Mode with 30% Increase in Torsional Inertia (CH-34).

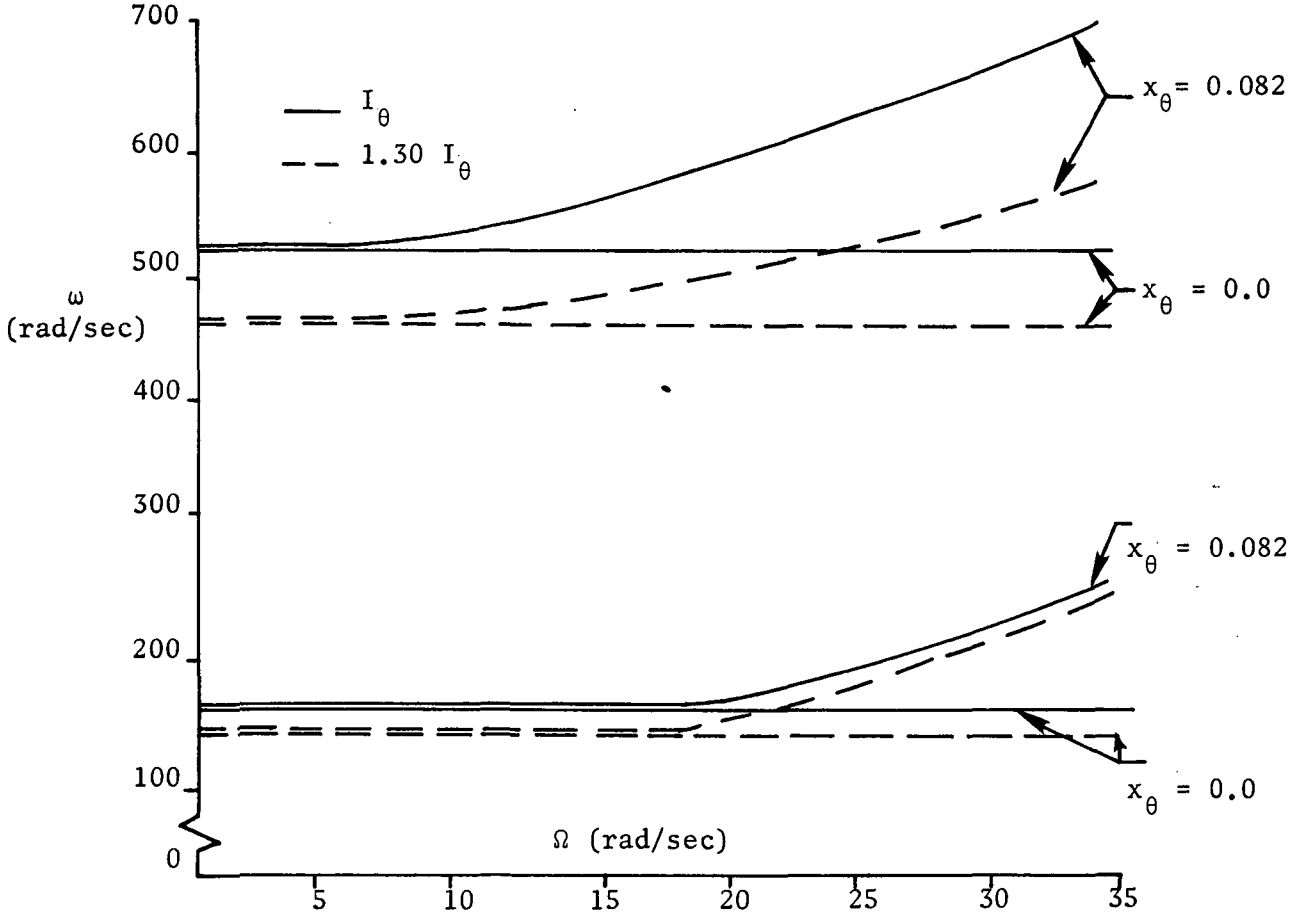

Fig. 15 Variation of Torsional Frequencies with 30% Increase in Torsional Inertia (CH-34).

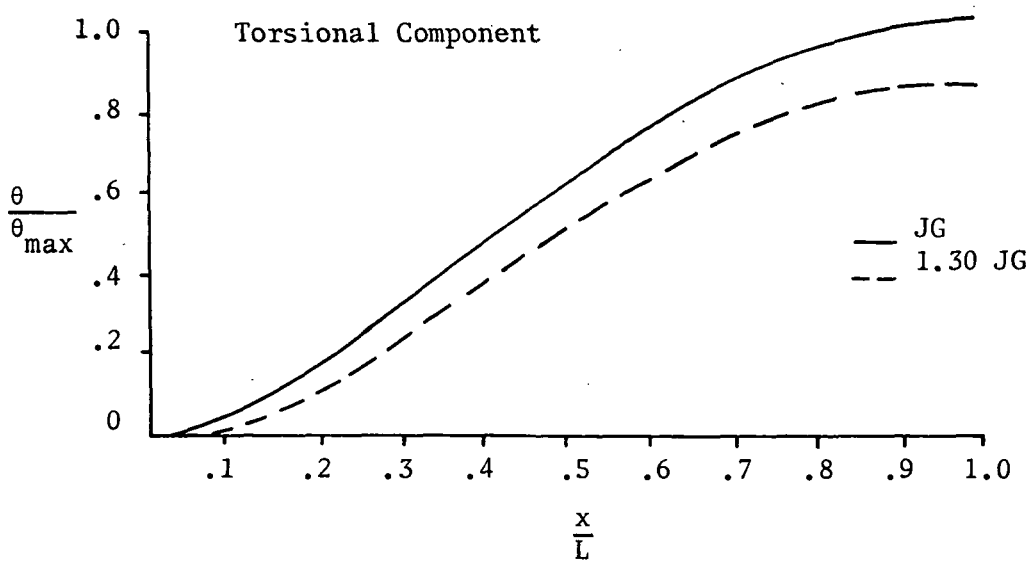

Fig. 16 Variation of First Coupled Mode with 30% Increase in Torsional Rigidity (CH-34).

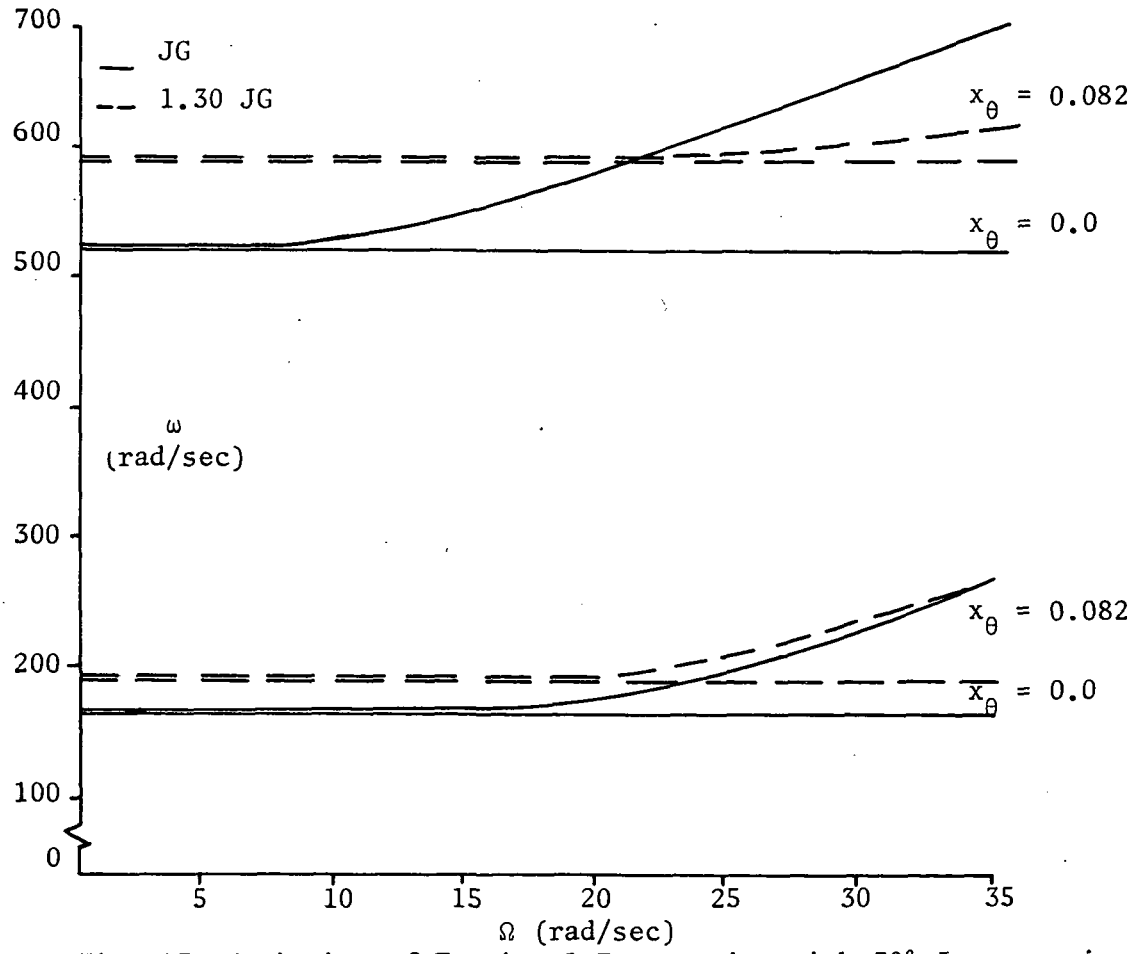

Fig. 17 Variation of Torsional Frequencies with 30% Increase in Torsional Rigidity (CH-34)

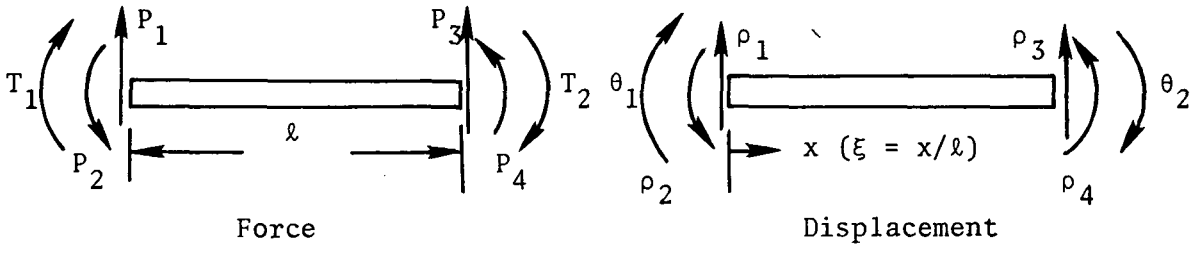

Fig. 18 Nodal Forces and Displacements for a Blade Element in Bending and Torsion.

NATIONAL AERONAUTICS AND SPACE ADMINISTRATION
WASHINGTON, D.C. 20546

OFFICIAL BUSINESS
PENALTY FOR PRIVATE USE $300

SPECIAL FOURTH-CLASS RATE BOOK

POSTAGE AND FEES PAID
NATIONAL AERONAUTICS AND SPACE ADMINISTRATION
451

U.S.MAIL

POSTMASTER: If Undeliverable (Section 158 Postal Manual) Do Not Return

"The aeronautical and space activities of the United States shall be conducted so as to contribute . . . to the expansion of human knowledge of phenomena in the atmosphere and space. The Administration shall provide for the widest practicable and appropriate dissemination of information concerning its activities and the results thereof."

—NATIONAL AERONAUTICS AND SPACE ACT OF 1958

NASA SCIENTIFIC AND TECHNICAL PUBLICATIONS

TECHNICAL REPORTS: Scientific and technical information considered important, complete, and a lasting contribution to existing knowledge.

TECHNICAL NOTES: Information less broad in scope but nevertheless of importance as a contribution to existing knowledge.

TECHNICAL MEMORANDUMS: Information receiving limited distribution because of preliminary data, security classification, or other reasons. Also includes conference proceedings with either limited or unlimited distribution.

CONTRACTOR REPORTS: Scientific and technical information generated under a NASA contract or grant and considered an important contribution to existing knowledge.

TECHNICAL TRANSLATIONS: Information published in a foreign language considered to merit NASA distribution in English.

SPECIAL PUBLICATIONS: Information derived from or of value to NASA activities. Publications include final reports of major projects, monographs, data compilations, handbooks, sourcebooks, and special bibliographies.

TECHNOLOGY UTILIZATION PUBLICATIONS: Information on technology used by NASA that may be of particular interest in commercial and other non-aerospace applications. Publications include Tech Briefs, Technology Utilization Reports and Technology Surveys.

Details on the availability of these publications may be obtained from:

SCIENTIFIC AND TECHNICAL INFORMATION OFFICE

NATIONAL AERONAUTICS AND SPACE ADMINISTRATION

Washington, D.C. 20546